Algorithms for Wireless Communication Systems Using SDR Platform

A thesis submitted to the
Graduate School of Natural and Applied Sciences

by

Hisham Fadl Allah M. Abuella

in partial fulfillment for the
degree of Master of Science

in

Electronics and Computer Engineering

This is to certify that we have read this thesis and that in our opinion it is fully adequate, in scope and quality, as a thesis for the degree of Master of Science in Electronics and Computer Engineering.

APPROVED BY:

Assist. Prof. Mehmet Kemal Özdemir ..... 
(Thesis Advisor)

Assist. Prof. Hakan Doğan .....

Assist. Prof. Tansal Güçlüoğlu .....

This is to confirm that this thesis complies with all the standards set by the Graduate School of Natural and Applied Sciences of İstanbul Şehir University:

DATE OF APPROVAL:

SEAL/SIGNATURE:

Declaration of Authorship

I, Hisham Fadl Allah M. ABUELLA, declare that this thesis titled, 'Algorithms for Wireless Communication Systems Using SDR Platform' and the work presented in it are my own. I confirm that:

- This work was done wholly or mainly while in candidature for a research degree at this University.
- Where any part of this thesis has previously been submitted for a degree or any other qualification at this University or any other institution, this has been clearly stated.
- Where I have consulted the published work of others, this is always clearly attributed.
- Where I have quoted from the work of others, the source is always given. With the exception of such quotations, this thesis is entirely my own work.
- I have acknowledged all main sources of help.
- Where the thesis is based on work done by myself jointly with others, I have made clear exactly what was done by others and what I have contributed myself.

Signed: Hisham Fadl

Date: 5 December 2016

Algorithms for Wireless Communication Systems Using SDR Platform

Hisham Fadl Allah M. Abuella

Abstract

This thesis presents a detailed study on software based channel emulators and a set of algorithms pertaining to the soft emulator. With the fact that several wireless communications technologies were released in the last decades, there are a lot of challenging issues emerging due to the need for faster and more reliable technologies. From these challenging issues, we have chosen to focus our research on two outstanding challenges: real-time software channel emulator and automatic modulation classification.

Recently, there has been an increase in the demand for a reliable and low-cost channel emulator to study the effects of real wireless channels. Hence, in the first part of the thesis, we discuss an implementation of a real-time software channel emulator. The real-time fading channel emulator was implemented by using a software defined radio platform. In order to verify the model, the frequency spectrum specifications of the channel generated was checked with a double tone transmitter. Then as a second step of verification, bit error rate (BER) of a real-time Orthogonal Frequency Division Multiplexing system using the Universal Software Radio Peripheral (USRP) and LABVIEW software was compared with the BER floor calculated from the theoretical equations. It has been shown that the developed channel emulator can indeed emulate a fading wireless channel.

In the second part of the thesis we focused on covering an issue related to blind estimation or classification of a parameter in wireless communications at the receiver. This problem appears in cognitive radios and some defense applications where the receivers needs to know the type of the modulation of an incoming signal. The efficient automatic modulation classification scheme proposed in this study can be utilized for a group of digitally modulated signals such as QPSK, 16-PSK, 64-PSK, 4-QAM, 16-QAM, and 64-QAM. We performed the classification in two stages: first we classified the modulation between QAM and PSK signaling, and then we determined the M-ary order of the modulation by developing Kernel Density Estimation and analyzing the probability density distribution for the real and imaginary parts of the modulated signals. Simulations were carried out to evaluate the performance of the proposed scheme for flat channels.

Thus, in this thesis first of all we were able to develop a software based channel emulator. The developed channel emulator can be a very useful tool for other researchers in testing

their real-time systems on a verified Doppler channel. Moreover, the emulator can find other applications from education to wireless device developments due to its flexibility. On the other hand, with the automatic modulation classification, the unknown modulation of an incoming signal can be determined. Hence, the two issues can be combined to find applications in cognitive radio developments.

Keywords: Channel Emulator, USRP, Automatic Modulation Classification, SDR

Yazılım Tabanlı Radyo Platformu Kullanan Kablosuz Haberleşme Sistemleri çin Algoritmalar

Hisham Fadl Allah M. Abuella

Öz

Bu tezde yazılım tabanlı kanal emülatörleri için detaylı bir çalışma ve bu emülatörlerde kullanılabilecek bir dizi algoritma sunulmuştur. Son birkaç on yıllık zaman zarfında bir takım kablosuz haberleşme teknolojilerinin piyasaya sürümü gerçeğinden yola çıkarak, daha hızlı ve gürbüz teknolojilerin geliştirilmesi esnasında birçok zorluklar ortaya çıkmaktadır. Bu zorluklar arasında biz öne çıkan iki zorluğu seçtik: gerçek zamanlı yazılım tabanlı kanal emülatörü ve otomatik kipleme sınıflandırılması.

Son zamanlarda gürbüz ve düşük maliyetli kanal emülatörleri gerçek zamanlı kablosuz kanalların etkisini çalışmak için talep edilmektedirler. Bu nedenle bu tezin ilk kısmında biz gerçek zamanlı yazılım tabanlı bir kanal emülatörünü tartışacağız. Gerçek zamanlı ve sönümlemeli kanal emülatörü yazılım tabanlı bir telsiz platformu ile uygulandı. Geliştirilen modeli doğrulamak için elde edilen kanalın frekans tayfı iki tane ton gönderen bir verici ile kontrol edildi. Daha sonra ikinci bir doğrulama için dikey frekans bölmeli çoklama tabanlı bir sistemin bit hata oranları yazılım tabanlı radyo, USRP, ve LABVIEW yardımıyla elde edilerek teorik değerlerle karşılaştırıldı. Bu doğrulamalar neticesinde geliştirilen kanal emülatörünün kablosuz bir kanalı gerçekte emüle ettiği gözlemlendi.

Tezin ikinci kısmında ise bir kör kestirim algoritması olan ya da kablosuz haberleşme alıcılarında parametrelerin sınıflandırılması kestirimini problemine odaklandık. Bu problem aynı zamanda kavramsal radyolarda ve bazı savunma sanayi uygulamalarında alıcının gelen sinyalin kiplemesini bilmesini gerektiren durumlarda da görülmektedir. Bu çalışmada geliştirilen etkili otomatik kipleme sınıflandırma algoritması yaklaşımı bir grup sayısal kipleme için kullanılabilir ki bu kiplemeler QPSK, 16-PSK, 64-PSK, 4-QAM, 16-QAM, ve 64-QAM olabilir. Yaklaşım olarak sınıflandırmayı iki aşamada gerçekleştirdik: önce QAM ve PSK sinyalleri için kipleme sınıflandırmasını gerçekleştirdik, ve daha sonra kiplemenin derecesini Kernel Yoğunluklu Kestirim yaklaşımını geliştirerek ve de gelen sinyalin reel ve sanal kısımlarının olasılık dağılım fonksiyonlarını analiz ederek elde ettik. Gerçekleştirdiğimiz simülasyonlarla kestirim algoritmasının performansı düz sönümleme kanalları için başarılı bir şekilde test edildi.

Sonuç olarak bu tezde öncelikle bir yazılım tabanlı kanal emülatörü tasarımı gerçekleştirdik. Geliştirilen kanal emülatörü gerçek zamanlı sistemlerini Doppler etkili kanallarda test etmek isteyen isteyen diğer araştırmacılar için çok faydalı bir platform sunabilir. Bunun yanında emülatörün tasarımı esnek olduğundan eğitimden kablosuz ürün tasarımı yapan yerlere kadar uygulama alanları bulabilir. Diğer taraftan da otomatik kipleme sınıflandırması ile bilinmeyen bir sinyalin kiplemesi belirlenebilir. Bu iki çözüm kavramsal radyodaki bazı zorlukların aşılmasında kullanılabilir.

Anahtar Sözcükler: Kanal emülatörü, USRP, Otomatik Kipleme Sınıflandırılması, Yazılım Tabanlı Radyo

To my parents, my sister and future love.

Acknowledgments

First of all, I want to express my gratitude to my advisor Prof. Kemal Özdemir for his endless guidance during my MSc. studies, for his patience, encouragement, and vast knowledge. His guidance aided me during my research and the editing of the papers. His advices especially personal ones are greatly valued. I could not have dreamed of having a better advisor for my MSc. studies. Thanks for helping me to continue my dream of pursing my PhD studies in USA. Also, I would like to thank my colleague helped me a lot especially in the channel emulator part.

Secondly, I would like to thank my thesis committee: Assist. Prof. Hakan Doğan and Assist. Prof. Tansal Güçlüoğlu for their helpful comments.

Last but not the least, I would like to thank my family in Egypt: my parents and sister for backing me and their endless encouragement. Also, I extend my thanks to my family in Turkey as they have made it feel like home.

Contents

List of Figures

Abbreviations

SDR	**S**oftware **D**efined **R**adio
BER	**B**it **E**rror **R**ate
QPSK	**Q**uadrature **P**hase **S**hift **K**eying
PSK	**P**hase **S**hift **K**eying
QAM	**Q**uadrature **A**mplitude **M**odulation
USRP	**U**niversal **S**oftware **R**adio **P**eripheral
FPGA	**F**ield **P**rogrammable **G**ate **A**rray
DSRC	**D**edicated **S**hort **R**ange **C**ommunication
UWB	**U**ltra **W**ide **B**and
RF	**R**adio **F**requency
LTE	**L**ong **T**erm **E**volution
CDMA	**C**ode **D**ivision **M**ultiple **A**ccess
FIR	**F**inite **I**mpulse **R**esponse
MIMO	**M**ultiple **I**nput **M**ultiple **O**utput
RMS	**R**oot **M**ean **S**quare
PER	**P**acket **E**rror **R**ate
EVM	**E**rror **V**ector **M**agnitude
AMC	**A**utomatic **M**odulation **C**lassification
PSD	**P**ower **S**pectral **D**enisty
GMM	**G**aussian **M**ixture **M**odel
ANN	**A**rtificial **N**eural **N**etwork
KDE	**K**ernel **D**ensity **E**stimation
CDF	**C**umulative **D**istribution **F**unction
PDF	**P**robability **D**ensity **F**unction
SNR	**S**ignal **N**oise **R**atio
LOS	**L**ine **O**f **S**ight

ML	**M**aximum **L**ikelihood
OFDM	**O**rthogonal **F**requency **D**ivision **M**ultiplexing
IFFT	**I**nverse **F**ast **F**ourier **T**ransform
FFT	**F**ast **F**ourier **T**ransform
ICI	**I**nter **C**arrier **I**nterference
SIR	**S**ignal **I**nterference **R**atio
HPF	**H**igh **P**ass **F**ilter
DFT	**D**iscrete **F**ourier **T**ransform
MSK	**M**inimum **S**hift **K**eying
FSK	**F**requency **S**hift **K**eying

Chapter 1

Introduction and Literature Review

In this chapter, the underlying facts of choosing the topics of this thesis will be presented. Then, the state of art for the algorithms of this study on common wireless communication issues will be discussed. For these first, different structures used for channel emulator will be presented. Then, a literature review on previous studies related to automatic modulation classification scheme will be given. At the end of the chapter, the rest of the thesis structure will be articulated.

1.1 Channel Emulators

Recent developments in the mobile wireless standards and technologies require researchers to have fast and economical ways of testing their work. Realistic channel scenarios are needed to test the performance of the new devices and ideas. This is where the importance of a well tested and verified channel emulator appears. As depicted in Figure 1.1, once the phase of testing the algorithms is fast, flexible and/or low-cost, the overall process of designing the standards and technologies will be faster and more economical.

As shown in Figure 1.2, the channel emulator replaces the real time channel in the transceivers system. Channel emulators are divided mainly into two main categories: hardware-based and software-based. Hardware-based channel emulators tend to be fast and have higher bandwidth, but are harder to modify. Software-based channel emulators are little slower since they usually need to down-convert the signal, apply the channel in base-band and finally up-convert the signal again. However, their advantage is that

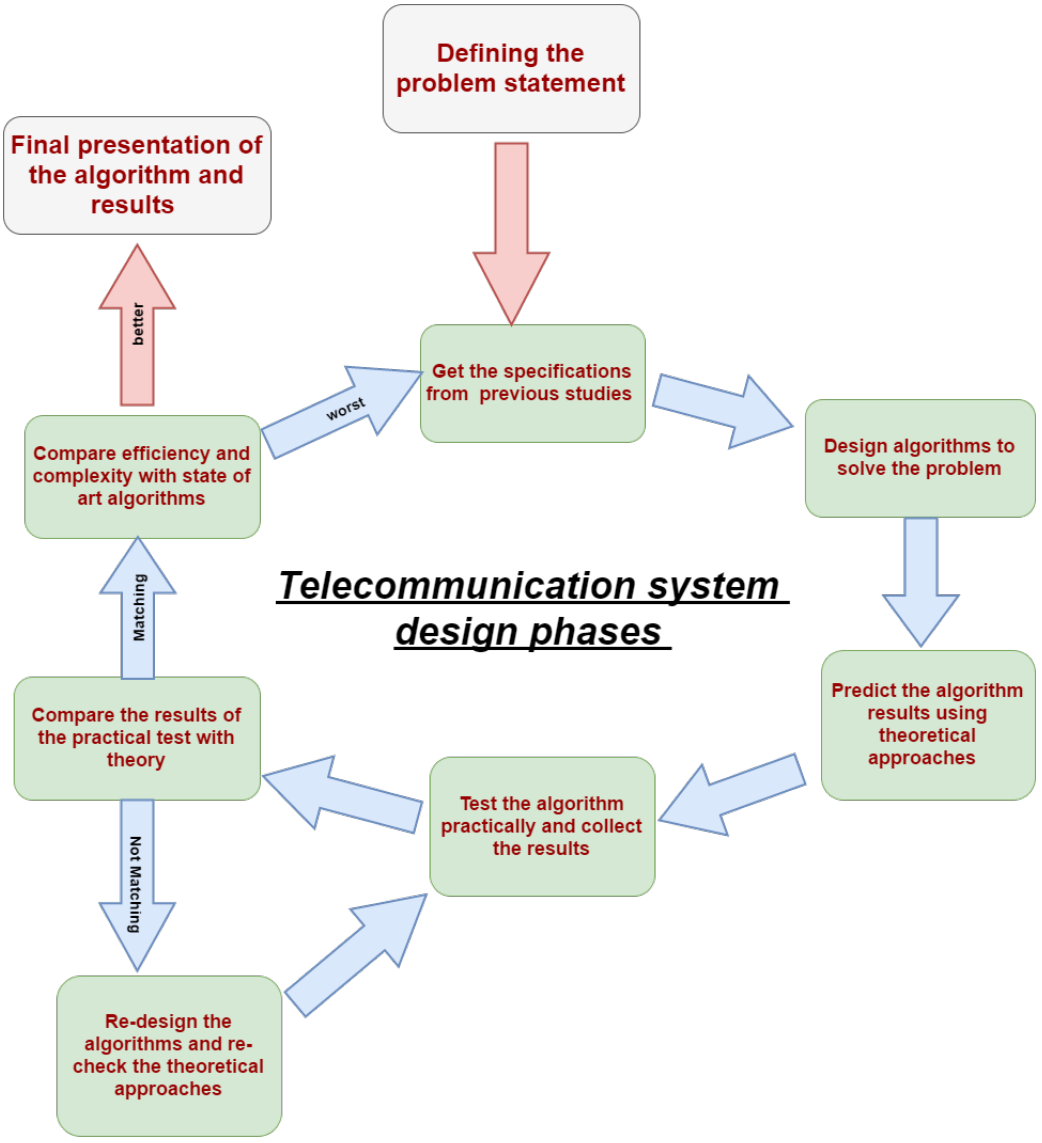

FIGURE 1.1: A Block diagram to present the phases of telecommunication system design.

whenever researchers need to change the channel scenario, it is just an update in the software without the need to change any hardware. In this work, we adopt the software-based emulator based on software defined radio (SDR) platforms.

Developing an easy to use, low-cost, and flexible channel emulator approach without buying a new device or tool is pivotal for the evolution of the mobile telecommunication research. It will allow researchers to test their ideas on real-time fading channels in a fast manner. Hence, the development of SDR-based channel emulators has become an important topic. Therefore, we observe a lot of studies on this topic such as the one in [2], where authors designed a SDR-based channel simulator using field-programmable gate array (FPGA) for testing baseband transceivers specific for standards of dedicated

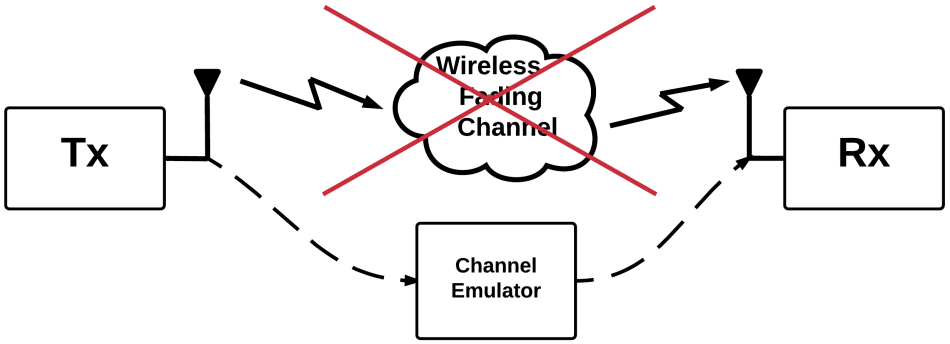

FIGURE 1.2: A Block diagram to describe the use of channel emulators.

short-range communications (DSRC) and ultra wide-band (UWB) systems. This system is just too specific for a given platform.

In a study specific to Wi-Fi systems, [3], a SDR-based real-time wireless channel emulator using FPGA has been proposed. Using the 802.11p protocol, the study evaluated the performance of modems for wireless vehicular communications using packet error rate. In [4], an affordable RF channel emulator for geostationary satellite transmission was developed but it was only targeting satellite transmission channels. Finally, in [5] the design and prototype implementation of a real-time FPGA-based channel emulator for benchmarking vehicular modems was investigated. In their study, the authors verified their emulator by calculating the packet error rate which is not a reliable way for the verification of the channel emulator. Also, they did not compare the results to any theoretical baseline.

Some researchers focused on specific standards such as the wide-band real-time mobile channel emulator for CDMA systems [6] and the multi-terminal LTE testbeds [7]. They discussed some of the limitations they had in their study like the restrictions on the channel models used. Others used FPGA on a hardware programming level as in [8] ,[9] for its high speed performance, where a QAM modulator was integrated with the emulator. The work introduced by [10] can run till 40 MHz bandwidth.

Using FPGAs or FIR filters as in [11] is very useful in terms of the data rates. On the other hand, these platforms tend to be inflexible as it is hard and expensive to modify the hardware design. Finally, the recent studies are targeting designing emulators for MIMO systems for the latest standards as in [12] and [13]. Due to the complexity of MIMO channels, the performance of the channel emulator in terms of data rates supported is

affected, therefore it is better to use hardware-based channel emulator for these systems since it is more stable and faster compared to software-based ones.

One common ground for all of the previous emulator models is that they do not show strong theoretical verification for the performance of the emulator. Instead, for the verification of the emulators, these researches focus on finding the mean square error difference between the emulator time domain channel and the estimated channel as in [7]. This is unreliable as it depends on the estimation algorithm used and does not give enough indication of the emulator performance in a complete system at different data rates. Another option is comparing empirical measurements of the channel taps and RMS delay spread of the power delay profile with the spectra and RMS delay spread generated from the channel simulator as in[2]. This method requires empirical measurements which is not available for every channel. Hence, in this study we focus on justifying the channel emulator results through two phases: first we check the frequency spectrum characteristics of the produced channel as done in [6], and secondly we apply the fading channel with different Doppler frequencies and check the BER for an OFDM system developed on the same USRP. Some earlier studies have tried to verify their emulator performance using packet error rate (PER) as done in [3], [14], and [5] or using EVM as introduced in [4]. While PER is specific for certain standards, BER is more general and shows the whole system performance that take into account the hardware factors. To our best knowledge our work is the first USRP-based channel emulator that compares the BER performance with the theoretical studies, thereby enabling the comparison of different channels an easy task.

1.2 Automatic Modulation Classification

In the last decades many wireless communication technologies have been released either for defense or civilian usages [15, 16]. In some defense applications, the receiver needs to know the type of the modulation of an incoming signal. On the other hand, for systems like cognitive and software defined radio, the receivers require the knowledge of the type of modulation of the received signal. Commercial or defense related spectrum sensing applications also heavily rely on the modulation classification techniques [17]. The fast and correct automatic modulation classification (AMC) will improve the performance and reliability of cognitive systems and will be useful for defense applications. In Figure 1.3,

two different digital modulation schemes are presented to show how different they can be. In the figure, the modulated signals are shown without any noise added so it is easy to differentiate between 8-PSK and QPSK for this ideal case.

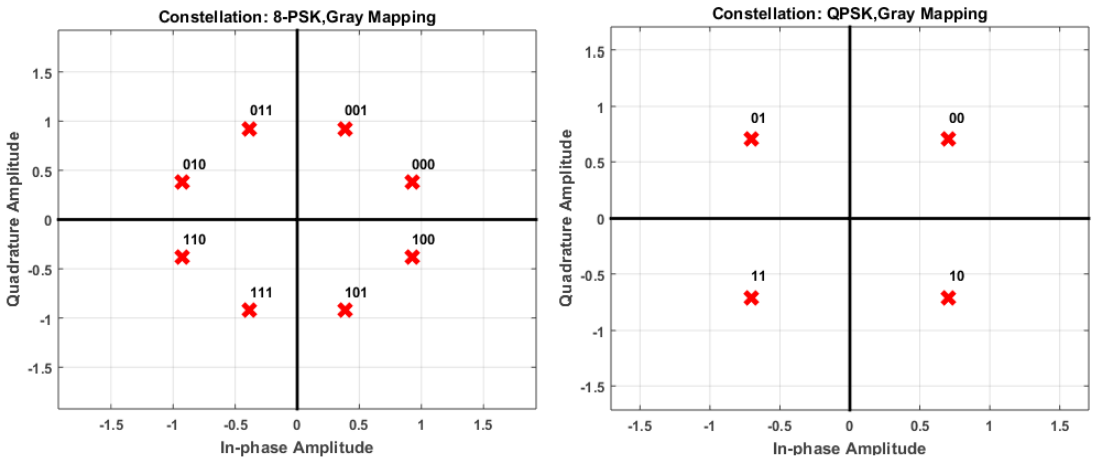

FIGURE 1.3: A comparison between different digital modulation techniques 8-PSK and QPSK.

Many studies have been performed to determine the best approaches for AMC. Proposed solutions are mainly divided into likelihood-based [18] -[19] and feature-based approaches [20] -[21]. When different approaches are on the table, it is important to identify the key parameters that reveal the merits of the proposed solutions. For AMC approaches, the main indicators of a good estimator are:

1. Number of features extracted from the received signal,
2. Complexity of the classifier used,
3. Assumptions made.

For features extraction, we can use many different techniques. For example, we can have computationally less heavy instantaneous approaches based on amplitude, phase, and power spectral density (PSD) of the incoming signal. Besides these, we can have computationally heavy statistical feature extraction approaches like mean, variance, magnitude, and location of the largest two peaks in the signal spectrum.

Similar to the case of feature extraction, for the classifier choices, we can also opt to use computationally heavy approaches such as ANN (Artificial Neural Networks) as in [22], GMM (Gaussian Mixture Models) as in [23] and KDE (Kernel Density Estimation)

as in [24] or just use decision trees [25]. On the other hand relatively less complex approaches like the distance properties between cumulative distribution functions (CDFs) corresponding to different modulation levels are studied [26]. These do not provide a good solution in terms of memory since we have to store the CDFs of the modulations techniques in different SNR values. Besides, the classification of new modulation techniques will increase the computations required.

Here, the most critical item is the list of assumptions made for the estimator. Like in many studies as stated in the survey [15], in our study too, we will assume perfect frequency offset and time offset recovery. We will also assume the channel to be frequency non-selective with Additive White Gaussian Noise (AWGN). The channel gain can be a constant or a Rayleigh fading component. Although some other studies assume a multipath channel and some additional impairments [20] -[27], here we keep the approach limited to single tap AWGN channels as we believe the typical application is for systems with line of sight communication (LOS).

Prior art differentiates QAM from PSK by using the signal's magnitude of fourth, sixth, and eighth order cyclic cumulants as features [28], [29]. To approximate the probability distribution of the features, the Gaussian mixture model was used as in [23] and [30]. Another approach was parameter estimation using GMM to set up an offline database and then to classify the received signal into different modulation schemes based on the existing database by using Kullback-Leibler (K-L) Divergence [20]. In another study maximum-likelihood (ML) decision theory to modulation identification was investigated [19], [30] and [31] where identification of modulations is based on the ML principle using only phase PDF information. The approach proposed in [32] is novel but can only work for binary modulation schemes. Similarly the approaches proposed in [28] and [33] are only applicable to m-PSK signals. A comprehensive approach proposed in [34] can cover different modulation types, but it is computationally heavy.

As pointed out in [17], it is very critical that the proposed modulation classification approaches bear low complexity when they are to be implemented in real applications. Therefore, in this study, as a way of decreasing the computational complexity of the modulation classification, we perform the estimation in two steps. Due to the simplicity and efficiency in comparison between QAM and PSK, in the first step we employ the variance of the absolute of the signal as the feature to decide whether its modulation is

QAM or PSK. Then, for the second step of the proposed method, we utilize KDE since it has been used successfully in areas such as statistical analysis and speech processing [20] -[35]. By representing the distribution of the signal of interest with a weighted sum of several multivariate Gaussian functions, KDE is used to get the probability density function (PDF) of the real and imaginary parts of the modulated signal for the m-QAM case, or the phase shift offset for the m-PSK case. The PDF functions are then used to determine the order of the modulation. In Figure 1.4 a one dimensional GMM is introduced to how a complex distribution can be represented in terms of a mixture of Gaussian functions where x represent the real and imaginary parts of the modulated signal in case of QAM signal.

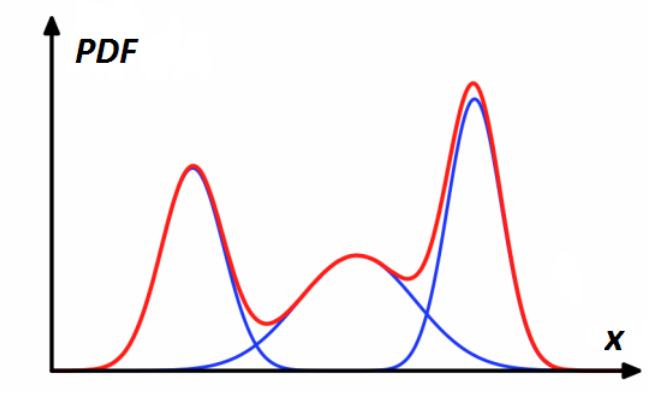

FIGURE 1.4: An example of a univariate (one dimensional) Gaussian mixture model. [1]

1.3 Conclusion

Here the motivations behind selecting the channel emulator topic have been revealed. Also, the channel emulators in previous studies especially SDR-based emulators were presented in detail. Software based channel emulators that are based on SDR platforms were not reported in previous studies. Therefore, in this thesis we will attempt to introduce such emulator, whose details are given in Chapter 3. In Chapter 4, a detailed study on automatic modulation classification algorithm is presented where the proposed algorithm is tested on AWGN and fading channels to calculate its performance for different channels. Finally, in the last chapter the concluding remarks and future directions are articulated. List of publications from the work of this study are also given in the last chapter.

Chapter 2

Real Time Fading Channel Emulator using SDR

2.1 Introduction

Wireless fading channel emulation is an essential ingredient for wireless communication technologies. It gives a way to test and verify the new algorithms and ideas proposed by researchers so that testing of the system efficiencies and performance in different situations is enabled. The use of emulators is more economic and time efficient than the costly field tests. Moreover, it can grant researchers with the results that are near to field test with the ability to change some parameters of the channel and repeat the test many times. This is why it is becoming more attractive and finding more usage in research and in the wireless industry.

There are two types of channel modeling mainly used by the academic society:

1. Physical wave propagation method (Ray Tracing)

   In this method, Maxwell equations are used to simulate the wave propagation in the location where we need to emulate the channel. Therefore, it needs detailed physical environment, geometry, and the dielectric properties. It is site-specific and gives accurate results at the cost of huge processing power. That's why they are typically run on servers. There is a lot of different programs for this type of simulations like Wireless InSite [36]

2. Statistical models method

   In this method, instead of taking the detailed physical environment, we use fading channel impulse responses to emulate the required channel with a certain statistical property. Real time fading channels can match a statistical model easily if the model is appropriately designed. What is needed to test the accuracy is to check the matching of the probability density function of the fading channel, power delay profile, and finally the auto/cross correlation of the channel. It needs less processing power than the physical wave propagation method. Hence, many researchers are now using it for its simplicity and efficiency.

Mainly, researchers need to measure the channel in real scenarios and assign statistical models for certain situations. There are different models based on the environment such as Indoor and Outdoor models. We are mainly focusing on emulating small-scale fading outdoor environment channels, as these channels are commonly used by researchers in the wireless communications field. Small-scale fading are fast changes in amplitudes, phases, or multipath delays of a radio signal over a short time or distance [37]. These changes are mostly due to the movement of the transmitter or the receiver, which will cause a Doppler shift and a change in the multipath delays and amplitudes at the receiver. Although this work is valid for multipath fading channels, we will focus on flat fading channels, since we would like to compare the simulation results with those of existing ones. Many statistical models for multipath fading channels have been proposed to predict the flat fading channels for outdoor environments. Clarke's Model for flat fading is a widely used model [38]. We will discuss the implementation of this model in more detail for our emulator given in Section 2.2.

The development of software defined radios is one of the most important breakthroughs in the telecommunication field. They were first introduced by Mitola in [39] and over the years many platforms have been developed. Standing out is the Universal Software Radio Peripheral (USRP) platform, which is a flexible and affordable SDR transceiver that turns a standard PC into a powerful wireless prototyping system. USRP platform was preferred due to its economical advantage since it is an available hardware that can be used easily. Moreover, it allows the use of high frequencies in the spectrum with larger bandwidth compared to other SDRs [40]. The ability to integrate ".m" (Matlab files)

and ".c" file scripts is also an advantage. A lot of libraries can be found online through NI community in [40].

To the authors' best knowledge, USRP-based channel emulators have not been widely discussed and evaluated in the previous research. Many commercial devices have been developed and tested to function as a channel emulator. For example, the work done by National Instruments in [41] is based on vector signal transceivers (VST). A lot of commercial emulators have been introduced by companies like Spirent and Keysights, the details of which can be found in [42] and Keysight in [43].

What differentiates this work from the prior art is that:

1. The strong verification scheme adopted.
2. Flexibility of the emulator as the channel model used can be modified easily.
3. With the suitable user interfaces, the emulator can be used as an efficient educational tool not just as a research tool.
4. Comparing the performance of different channel emulators is hard due to the different assumptions and parameters. However, comparing to the theoretical BER curves gives us a more common and reliable evaluation.

The rest of the chapter is organized as follows: In Section 2.2, we introduce the fading channels, their generation, and the exact model that we use. Then we present a small Subsection about our OFDM system specifications. In Section 2.3, we talk about the theory and equations of the BER curves that are used for comparison. Then, we present the setup of the USRP and the block diagram of OFDM transceiver used in the verification test. Finally, the results and some discussions are presented in Section 2.4.

2.2 Implementation of fading channels

In this Section we introduce the fading channel model that describes our system and the method of generating the channel for the software emulator. A lot of work has been done in modeling and generating different fading channel environments, since fading channels

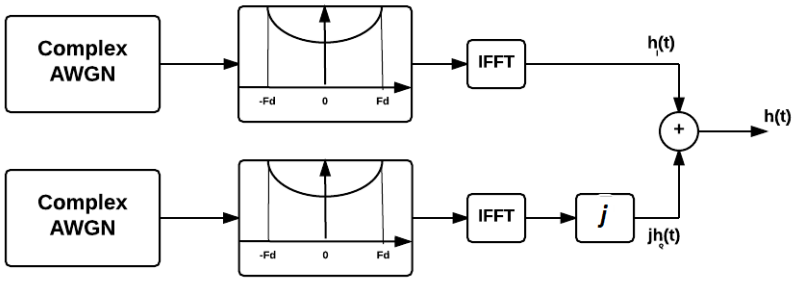

FIGURE 2.1: Clarke/Gans model to generate the fading channels.

are more realistic and better represent the real time channel environments than only using AWGN.

These models can be mainly divided into indoor and outdoor channel models. We focus our research on outdoor channel models. Filtered white Gaussian noise (FWGN) model is the most famous model where the white Gaussian noise is filtered by the desired Doppler filter either in time or frequency domain.

We have chosen filtering in frequency domain (Clarke/Gans model) since the length of the OFDM time symbol allows us to generate channel packets of the same length without the need for a continuous channel generation process. We can use the model introduced in [37] as shown in Figure 2.1. Another advantage is that this model is flexible and easy to implement since the desired Doppler filter can be modified easily.

Figure 2.1 shows a block diagram for the Clarke/Gans model, in which there are two identical branches: one for a real part and the other for an imaginary part of the channel. A complex Gaussian noise is first generated and filtered in the frequency domain by the desired Doppler filter. Then, the filtered noise is transformed into the time-domain by using an Inverse Fast Fourier Transform (IFFT) block. Note that the output of the IFFT is conjugate symmetric. At the end, to construct the complex fading channel, we add the real part to the imaginary part of the output. A detailed flow chart of the algorithm used with the USRP's is shown in Figure 2.2.

In Figure 2.2, N_d is the number of the samples of the transmitted signal, f_s is the sampling frequency of the signal (channel) and f_D is the maximum Doppler frequency used. Hence, as f_D increases the channel produced is more time-variant. N is the number of samples used in the frequency domain filtering. We take N to be a power of 2 since IFFT block is introduced to the output.

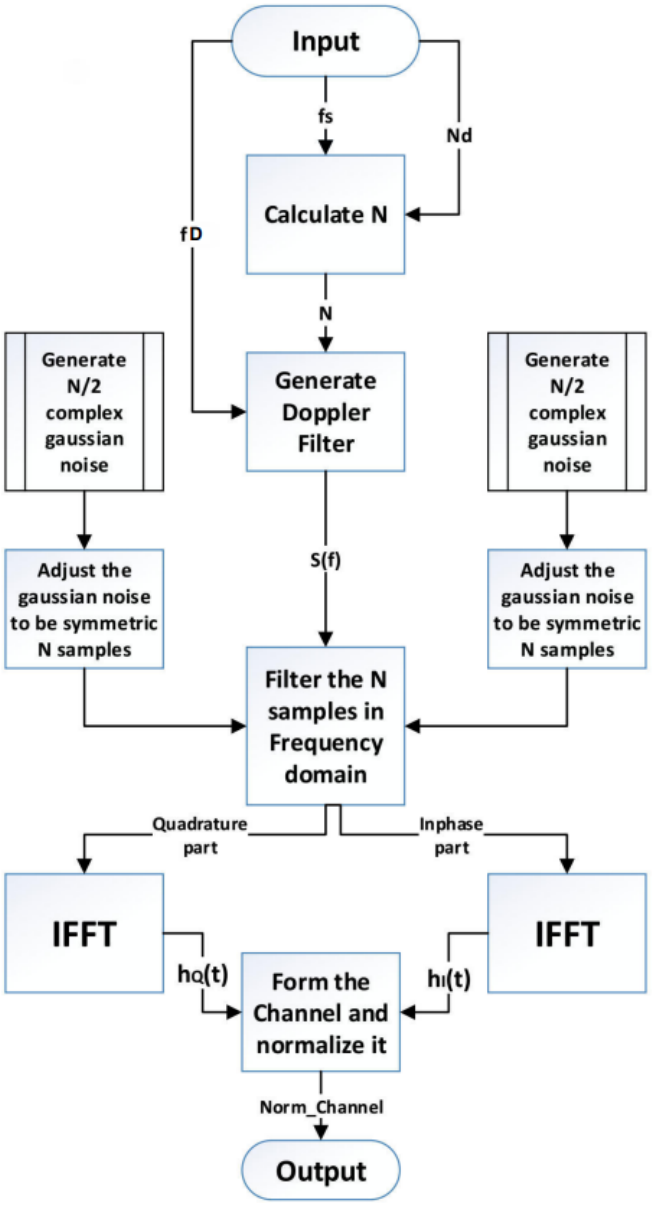

FIGURE 2.2: Flow diagram of the used Algorithm in Fading Channel Generator Block.

$S(f)$ represents the Doppler filter used. In our simulations, Clarke/Gans model was adopted from [38] and [44]. It assumes that scattering components around a mobile station are uniformly distributed with an equal power for each component.

where,

$$S(f) = \frac{1.5}{(\pi * f_D)\sqrt{(1-(f/f_D)^2)}} \tag{2.1}$$

Finally the final channel generated is as shown in Figure 2.2,

$$h = h_I - 1i * h_Q \tag{2.2}$$

2.2.1 Implementation of Multipath Doppler Channel

We stated that this work can be extended to multipath fading channels in the introduction. We will introduce a detailed block diagram and results to prove that our channel emulator can produce multipath fading channels. In Figure 2.3, we provide a detailed block diagram of the system used.

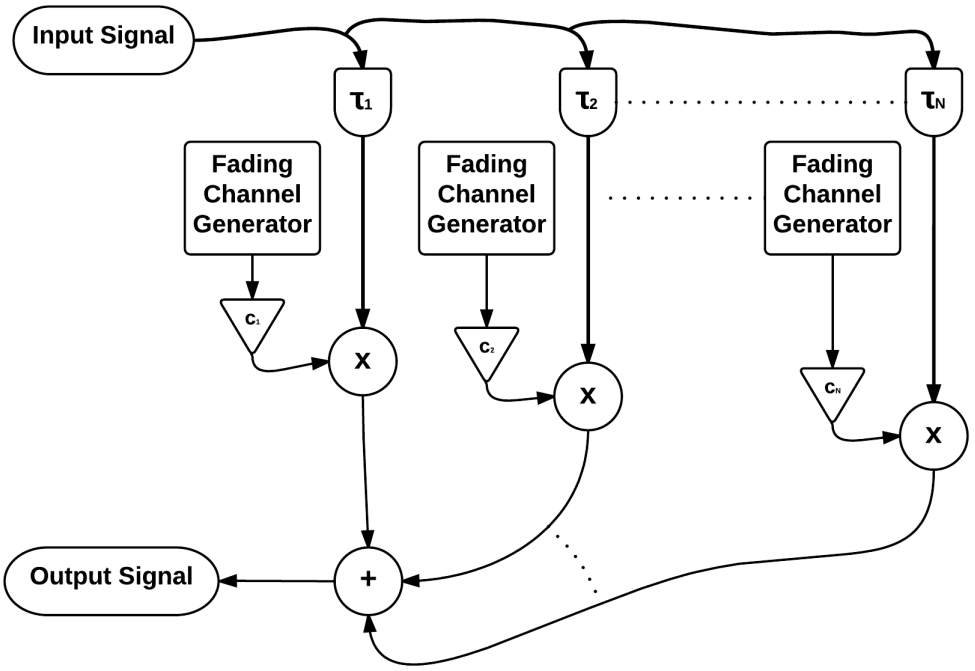

FIGURE 2.3: Block diagram to explain how to produce Multi-path fading channel.

Then, we can represent the output of the multipath fading channel block as in Eq. 2.3

$$r(t) = \sum_{i=1}^{M} c_i s(t - \tau_i) * h_i(t) + n(t) \tag{2.3}$$

In Figure 2.3, $r(t)$ is the received signal, $s(t-\tau_i)$ is the delayed input (transmitted) signal by delay τ_i seconds introduced to a multi-path channel with M taps with a gain c_i each and $n(t)$ is complex AWGN. Here, the samples of AWGN are distributed as $\sim \mathcal{N}(0, \sigma_n^2)$ where σ_n^2 is the noise variance. In case of a single tap channel (flat fading channel) M is equal 1 and for the case of only AWGN channel M and C_1 are equal 1 and τ_1 is zero, while in the case of non line of sight transmission τ_1 is not equal zero.

Since we would like to compare the simulation results with those of existing ones, we will only discuss flat channel (one tap channel) for the rest of the thesis. Finally, we present the simulation results of a multipath channel in Section 2.4.3.

2.2.2 Specifications of the OFDM system used in verification

An OFDM system based on a typical fixed WiMAX standard parameters has been used in the verification process of the channel emulator. Its specifications are as follows:

- It uses quadrature phase shift keying (QPSK), or it transmits 2-bits per sub-carrier with f_s=200 KHz.
- It is using 256 sub-carriers (N) per symbol.
- A 1/4 cyclic prefix, or 64 point cyclic prefix is used per OFDM symbol.
- At the receiver, Van De Beek algorithm [45] is used to detect the cyclic prefix locations for synchronization.
- At the receiver, equalization is done by linear fitting for both I and Q components using reference symbols, then we use LABVIEW block to map the symbols to bits.

In Figure 2.4, we present a detailed block diagram of the OFDM transceiver used in our simulations.

Although the use of an OFDM system allows us to test multipath fading channels, for the sake of simplicity and to make comparison of BER with the practical USRP results, we perform tests with for a flat fading channel. This will also allows us to use the theoretical equations as discussed Section 2.3.

2.3 Theoretical BER curves

It is very challenging to compare the theoretical BER equations with the results under the assumptions that are made by our channel emulator. Also there are a lot of additional errors caused by the hardware of the USRP. The variation in the complex channel gain introduced to the ODFM signal (which is the Doppler shift) causes loss of orthogonality of the sub-channels of the OFDM symbol, causing inter-carrier interference (ICI).

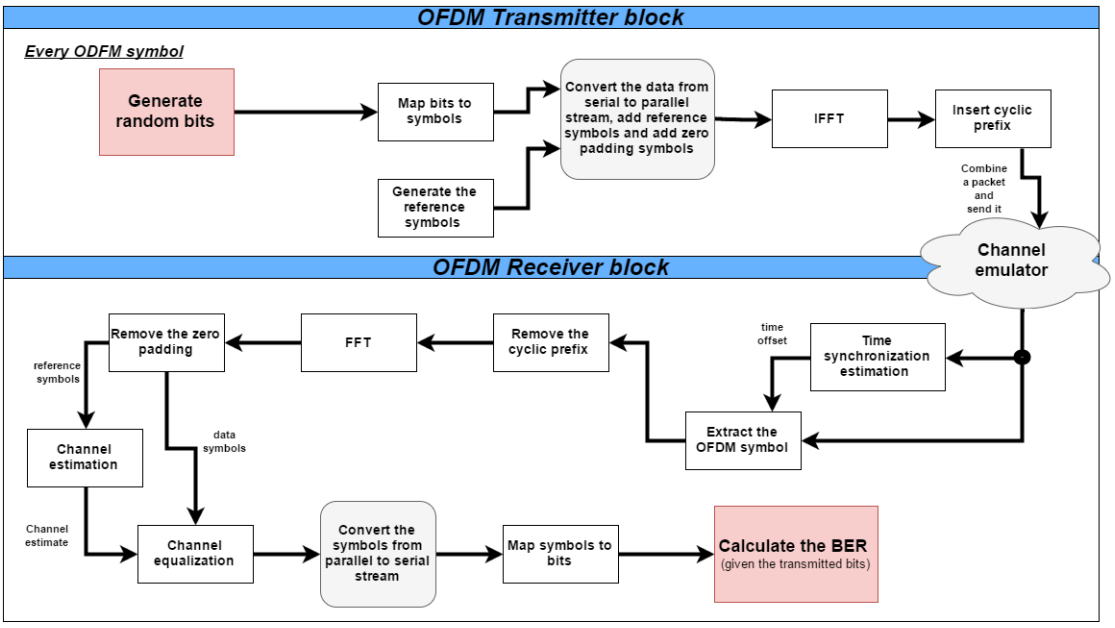

FIGURE 2.4: Block diagram to describe the OFDM used.

Introduction of Doppler shift causes ICI effect for the data. Using the results found in [46], we assume that ICI can be modelled as AWGN noise resulting in a noise floor at high SNRs. The ICI variance is as shown in Eq. 2.4, under the assumption that the Clarke's 2D isotropic scattering model with an isotropic antenna and normalized channel as in [46]:

$$\sigma_{ICI}^2 = \frac{E_{av}}{T} - \frac{E_{av}}{TN^2} * (N + 2\sum_{i=1}^{N-1}(N-i) * J_0(2\pi f_D T i)) \tag{2.4}$$

Therefore, ICI term is only a function of E_{av}, N, T and f_D, where E_{av} is the average energy in the OFDM Symbol, N is the number of sub-carriers in the OFDM symbol, T is the OFDM symbol duration as stated in [47] and $J_0(.)$ is the first order Bessel function. All the previous parameters are the OFDM communication system parameters while f_D is the maximum Doppler shift introduced by the fading channel. A detailed derivation for how to find the ICI due to Doppler shift can be found in Appendix A.

The signal to interference (SIR) level can be readily found by the following formula as [46]:

$$SIR = \frac{E_{av}/T}{\sigma_{ICI}^2} \tag{2.5}$$

By substituting the ICI variance into the well known BER equations in terms of Signal to interference ratio (SIR), we can calculate the BER_{Floor} for different cases of Doppler shift. In our study, as we used QPSK, the equation that will be used is [47]:

$$BER_{Floor} = Q(\sqrt{SIR}) \tag{2.6}$$

In Eq. 2.6, $Q(x)$ is the Q-function which is the probability that a normal random variable will be larger than x standard deviations above the mean.

Finally, in Figure 2.5, the BER curve floor (value at high SNRs where only ICI is affecting the BER) is shown for varying number of subcarriers. As shown in Figure 2.5, the curves are matching exactly with those given in [47]. As can be seen from Eq. 2.4, as the f_D increase the BER floor increase. Also, as the subcarriers number increase the power of the ICI term increase so it results an increase in the BER floor.

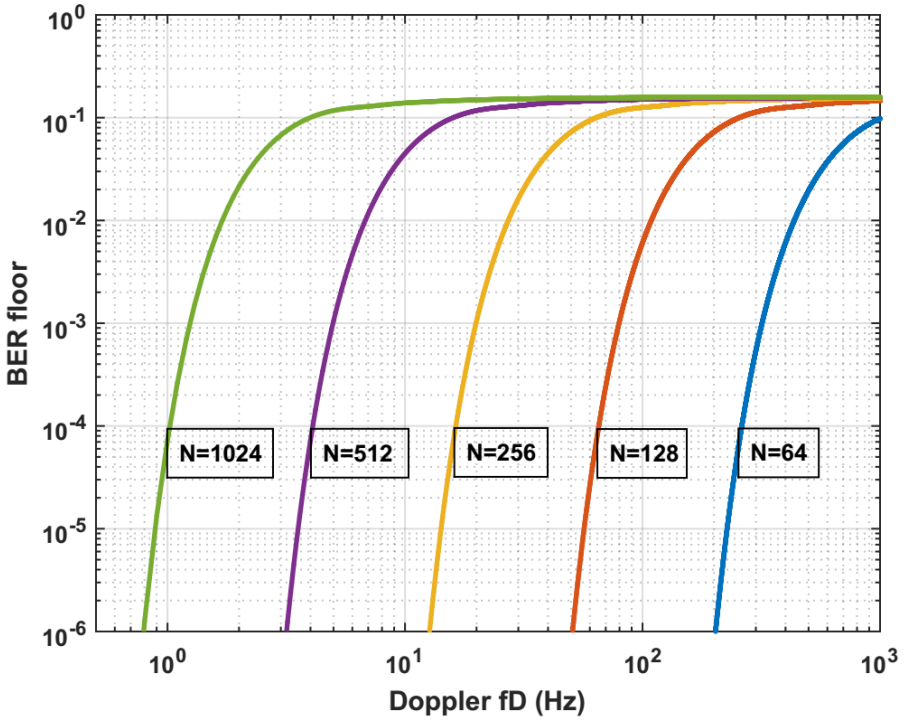

FIGURE 2.5: BER Floor for different N values when changing the Doppler frequency for QPSK OFDM system when R_b = 10 MHz.

2.4 Results

2.4.1 First verification phase

In the first phase, we check the fading channel spectrum characteristics using a single tone signal.

Figure 2.6 is a block diagram that shows how the USRP needs to be connected to perform the first phase of verification.

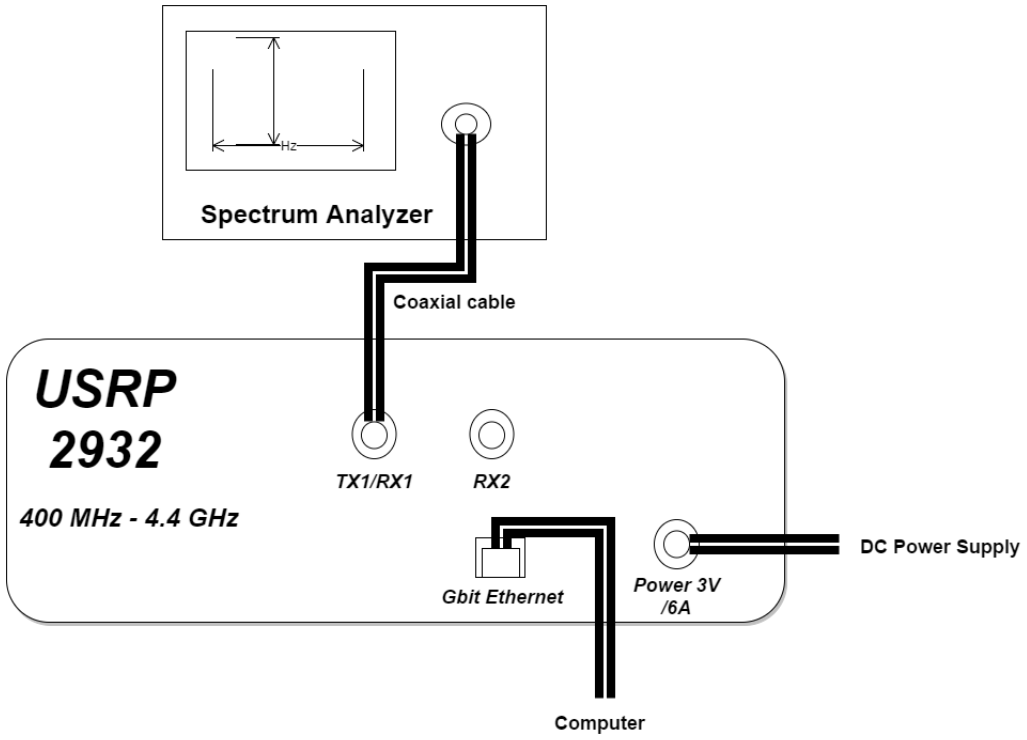

FIGURE 2.6: A block diagram to describe setup of the second phase of verification.

Figure 2.7 shows the setup of the USRP NI-2932 [48] and the Spectrum Analyzer used to verify the channel introduced to the single tone shown in Figure 2.8

The transmitter sends a single tone with f_m= 50 KHz. Ideally, when there is no channel, the spectrum analyzer shows only 2 Delta functions at $f_c \pm f_m$ as in Figure 2.8, where f_m is the maximum frequency in the signal and f_c is the carrier frequency. When the channel emulator applies the fading channel with f_D = 10 KHz, the result changes to the one shown in Figure 2.9. In this figure, both of the Delta functions take the U-shape of Clarke's model used in the channel generation with a BW = 20 KHz. BW is the separation between the two peaks in the Doppler shape which indicates the Doppler

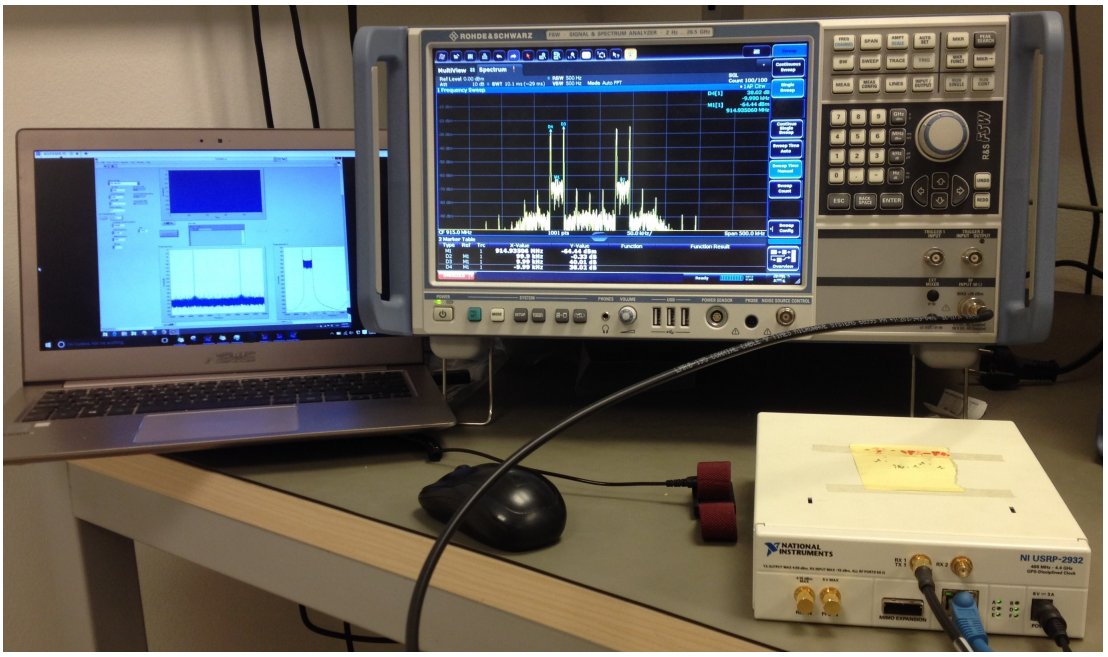

FIGURE 2.7: The Setup of the USRP and the Spectrum Analyzer.

spread. Finally, when changing f_D to 20 KHz, the Doppler shape bandwidth is doubled as shown in Figure 2.10.

These figures show that the behaviour of the spectrum of the signal is as expected, and hence these results can be used towards verifying the fading channel spectrum characteristics.

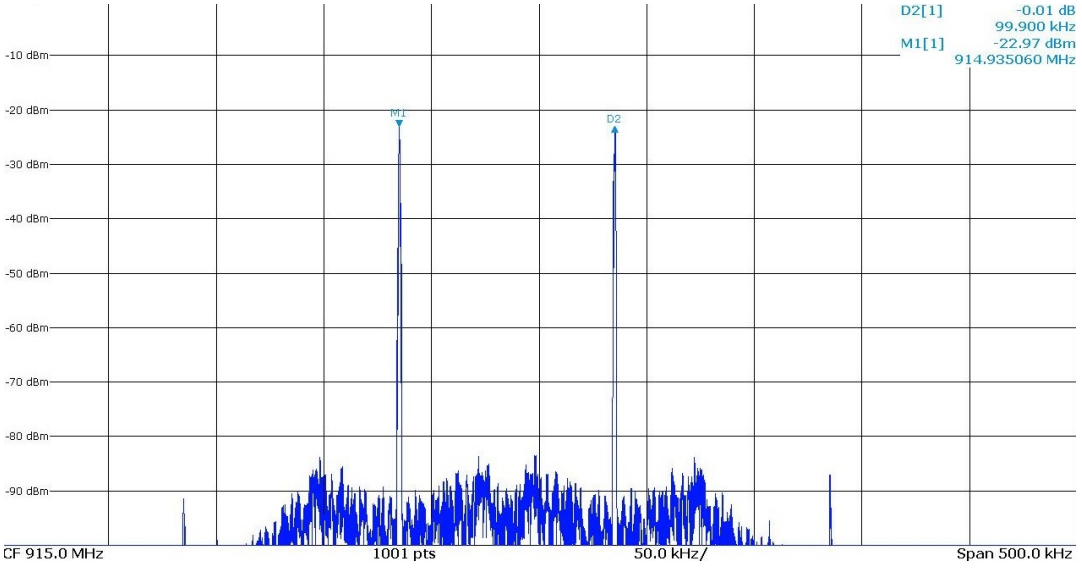

FIGURE 2.8: Results shown on the Spectrum Analyzer when the channel is idle

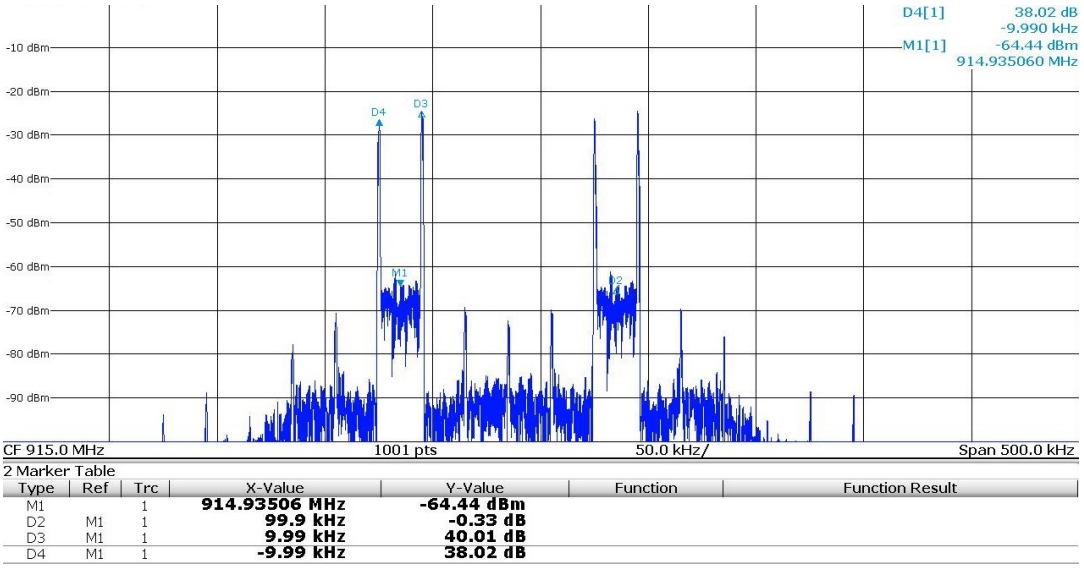

FIGURE 2.9: Results shown on the Spectrum Analyzer when the channel have f_D = 10 KHz

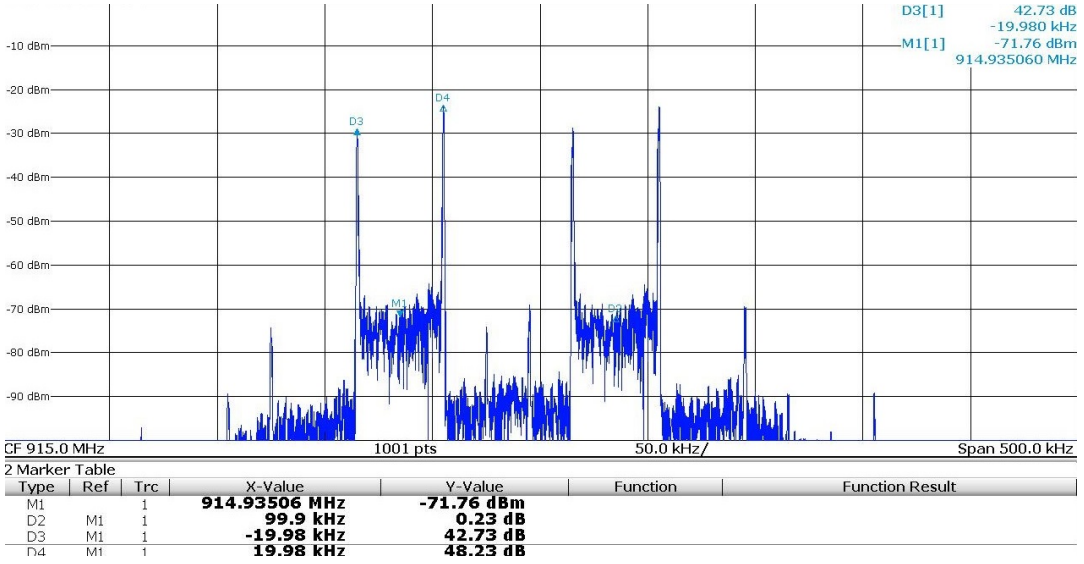

FIGURE 2.10: Results shown on the Spectrum Analyzer when the channel have f_D = 20 KHz

2.4.2 Second verification phase

In this phase, we verified the performance of the emulator by using an OFDM system. We compare the BER performance of our fading channel emulator with theoretical equations at different SNRs and Doppler shifts. The channel emulator is introduced after the transmitter block in the USRP but just before the receiver blocks.

First we present a simple block diagram to explain the real block diagram used in LABVIEW to get the results presented in Figure 2.14 and on how to control the USRP.

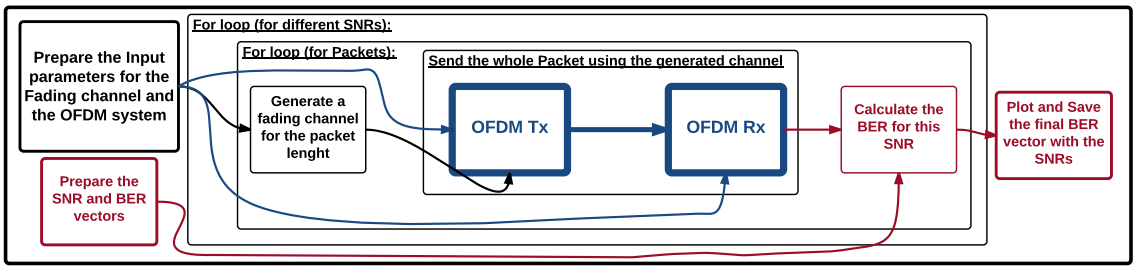

FIGURE 2.11: A simplified block diagram to describe the block diagram of the VI used to generate the BER Curves.

Figure 2.13 is showing the setup of the USRP used to generate the BER vs. SNR curves where transmitter (Tx) and receiver (Rx) ports are connected to each other by a coaxial cable. Also, the LABVIEW diagram and code to generate the fading channel is found in Appendix B.

Figure 2.12 is a block diagram that shows how the USRP connected to perform the second phase of verification where the USRP used is NI2932 [48].

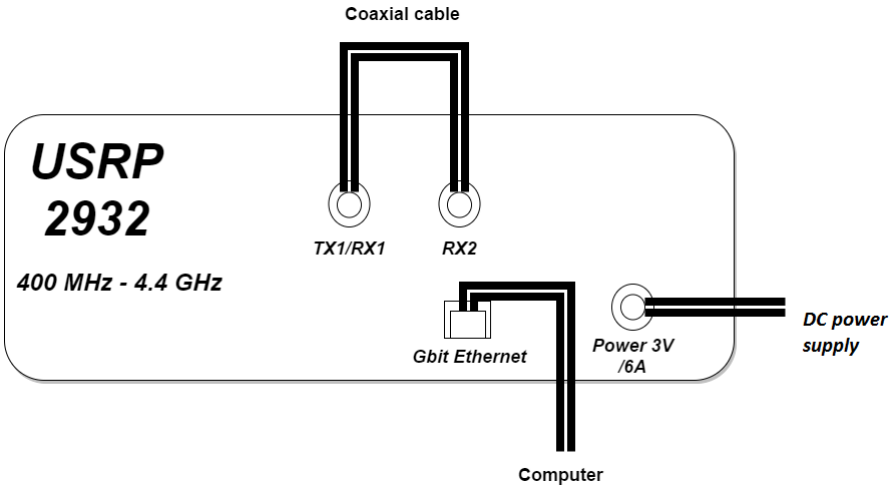

FIGURE 2.12: A block diagram to describe setup of the second phase of verification.

The results in Figure 2.14 shows the BER curves for different fading channels when using the OFDM system on the USRP and the theoretical BER curves for OFDM systems under fading channels.

As expected as the Doppler frequency increases the BER increase or it gets worse. Moreover, the BER floor is almost the same for the case of USRP emulation and MATLAB simulation. After the addition of the correction factors stated in Section 2.4.4 to the theoretical equations, we get Figure 2.15, which is the same curve in Figure 2.5. It is

FIGURE 2.13: The Setup of the USRP.

noticed that there is a difference between USRP results and theory which we think is a result of imperfections of the USRP or other imperfections from the integration of Matlab and USRP platforms.

2.4.3 Multipath channel simulation results

In this section we present the MATLAB simulations BER curves when f_D=10,50 Hz in Figure 2.17, for two multipath channel setup where Channel 1 power delay profile and Channel 2 power delay profile are presented in Figure 2.16.

In Figure 2.17, the BER curves are as expected as the second path power increase the system performance is worst since it acts now as a frequency selective fading channel, while in the case of channel 1 it is very near to the flat fading at the same Doppler frequency.

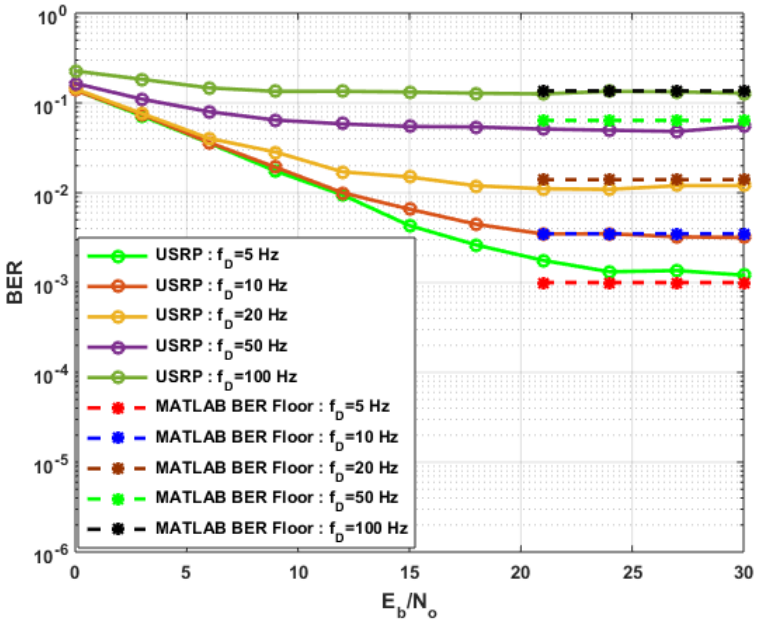

FIGURE 2.14: BER Curves for f_D=5,10,20,50,100 Hz when f_s=200 KHz for USRP and MATLAB simulation BER floor.

2.4.4 Sources of error and mismatch

There are lots of sources for the errors and mismatch between USRP results and the theoretical curves, since we are using a hardware USRP to emulate the OFDM system and the fading channel. First, we should consider the time synchronization error between the transmitter and receiver. Another source of error is the channel introduced to the signal in the coaxial cable connecting the Tx and Rx port in the USRP. Figure 2.14 shows that the BER curves generated by the USRP for each f_D case is worse than the theoretical curve for this f_D even after considering an addition of an error floor ICI due to the above error sources (-10dB). It was impossible to get a near curves without correcting the used f_D by a factor 16.

Some of the error sources were fixed directly, while the others we have used the correction factors above, we believe that these errors are the source of the correction factors.

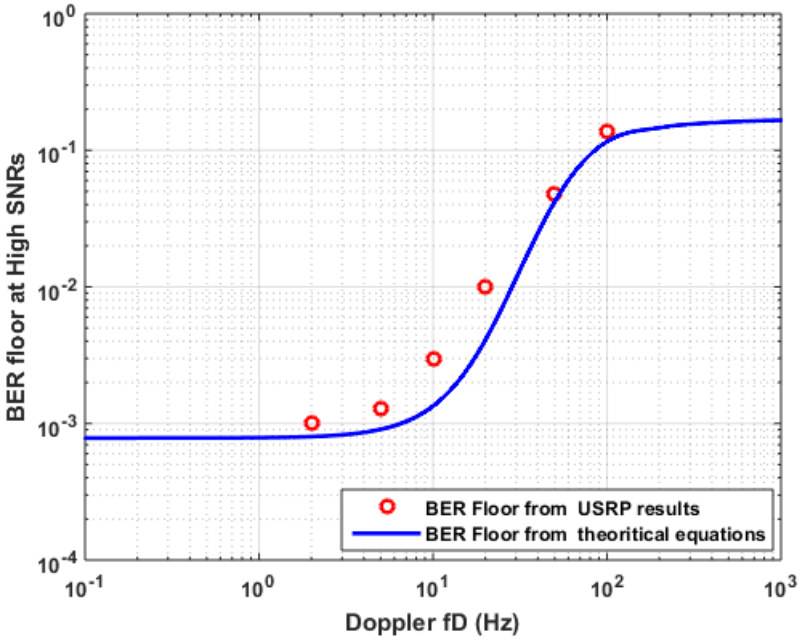

FIGURE 2.15: BER floor at f_D=2,5,10,20,50,100 Hz when f_s=200 KHz for USRP and Theoretical BER floor.

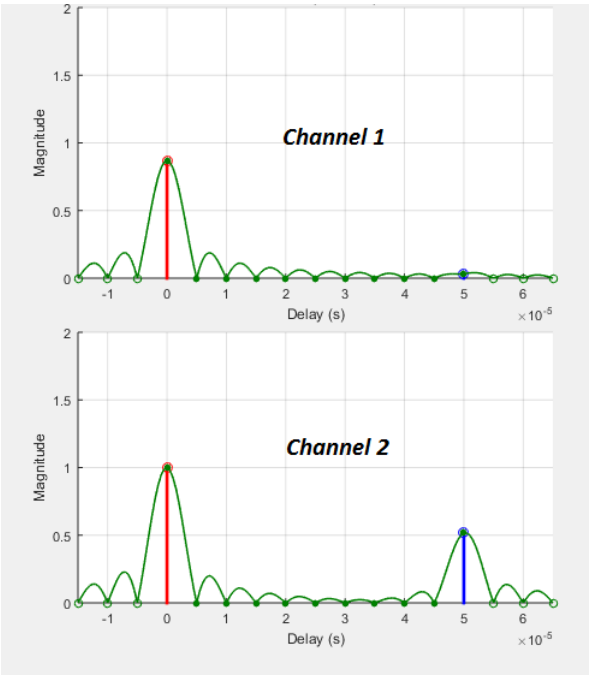

FIGURE 2.16: Channel 1 and Channel 2 power delay profiles.

2.5 Conclusion

In this chapter, we presented the software based channel emulator by using the USRP platform. The developed emulator was verified for the generation of the Doppler spectrum and the BER performance, where it is compared with the theoretical curves.

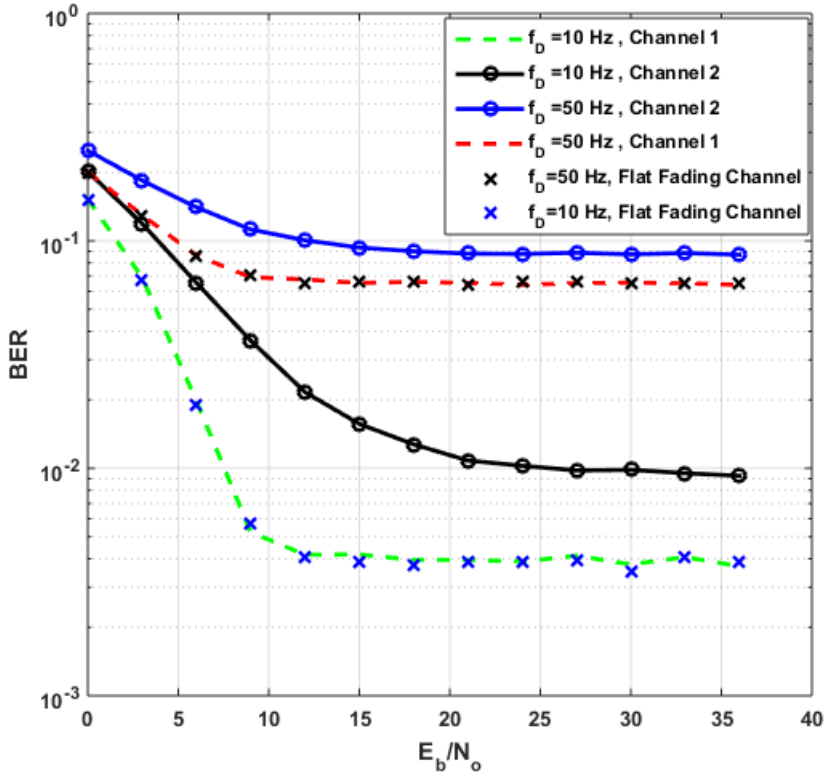

FIGURE 2.17: BER Curves for f_D=10,50 Hz when f_s=200 KHz for MATLAB simulation for 2 Multi-path channels.

Throughout this exercise we observed that the USRP can introduce some imperfections, which then needs to be compensated through some coefficients. With this, we have developed a software based channel emulator by using a SDR platform.

Chapter 3

Automatic Modulation Classification based on Kernel Density Estimation

3.1 Introduction

Automatic modulation classification (AMC) is a process of determining the modulation type of a signal. When known pilot data is not available from an incoming signal, then AMC is referred as blind AMC. We propose an efficient automatic modulation classification scheme for a group of narrow-band and digitally modulated signals such as QPSK, 16-PSK, 64-PSK, 4-QAM, 16-QAM, and 64-QAM. The classification was performed by analyzing the probability density distribution for the real and imaginary parts of the modulated signals.

There has been a lot of studies for the automatic modulation classification as discussed in Chapter 1, however what differentiates this work from the prior art is that:

1. A new amplitude and phase amplification technique for PSK is employed to estimate high order M-ary data.
2. Unlike the usage of an offline database, here the output of the KDE is exploited for calculation of the peaks that presents a straightforward differentiation between M-ary order signals.

3. Number of peaks calculation technique was introduced after the filtering of PDF, which has been obtained from the KDE technique.

4. Classification between QAM and PSK modulations using the variance of the signal amplitude was introduced.

3.2 System model

3.2.1 System model

In this study, the basic communication system model depicted in Figure 3.1 is taken as the reference model. The transmitter consists of data generation, modulation, and up-conversion, while the receiver is made up of down-conversion, synchronization part, channel compensation, AMC classification, and the demodulation parts. In this study, we assumed that up-conversion, down-conversion, and the time frequency synchronizations were already handled by different communication blocks.

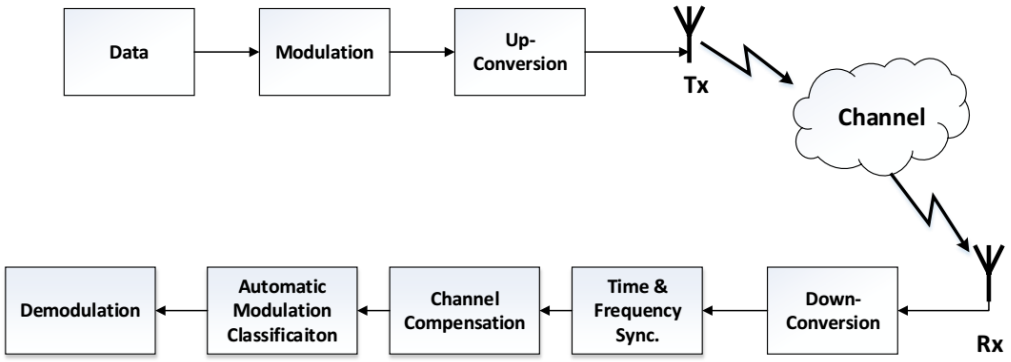

FIGURE 3.1: The reference system model.

3.2.2 Signal model

The received signal, which is down-converted and synchronized in time and frequency, for single tap channel can be written as:

$$y(n) = h * x(n) + w(n) \tag{3.1}$$

where h is a complex value. Its amplitude (channel influence factor) is Rayleigh distributed, while its phase is uniformly distributed between 0 and 2π with the assumption that h is constant through the whole classification phase (slow flat fading channel). Moreover, $w(n)$ is the complex AWGN and is distributed as $\sim \mathcal{N}(0, \sigma_w^2)$, or

$$f(w) = \frac{1}{\sigma_w \sqrt{2\pi}} e^{-(w)^2/2\sigma_w^2}. \tag{3.2}$$

Here $x(n)$ represents the transmitted baseband complex symbols and has a discrete uniform distribution with zero mean and unity variance. This assumption is justified since transmitters of wireless systems generally randomize the information bits, resulting in constellation points to be equiprobable and hence zero mean. The constellations are normalized so that the average energy is equal to unity. Then under these conditions the variance become the same as the average energy or unity, i.e.,

$$\hat{\sigma_y^2} = var\left[y(n)\right]. \tag{3.3}$$

Here we assume perfect channel estimation. In case the channel estimation is to be made part of the classification process, the blind channel estimation algorithms introduced in the following references could be exploited [49], [50], and [51].

After channel estimation block we compensate the received symbols by the following equation.

$$\hat{y} = \frac{h * x(n) + w(n)}{h_{estimated}}. \tag{3.4}$$

Assuming the $h_{estimated}$ is perfect, we get

$$\hat{y} = x(n) + \frac{w(n)}{h_{estimated}}. \tag{3.5}$$

Assuming that $x(n)$ and $w(n)$ are uncorrelated, one can get:

$$\sigma_y^2 = \sigma_x^2 + \frac{\sigma_w^2}{\sigma_h^2}, \tag{3.6}$$

where σ_h^2 is the $abs\left(h\right)^2$ (channel power), and

$$\sigma_x^2 = 1 \qquad (normalized) \tag{3.7}$$

We can then estimate the noise power, to be used by the KDE, by using the following equation:

$$\hat{\sigma_w^2} = (var(y(n)) - 1) * \sigma_h^2. \tag{3.8}$$

Since the expected value of $y(n)$ is zero, the variance of $y(n)$ is then simply the expected value of $y(n)^2$, or $E\left[y(n)^2\right]$.

3.2.3 KDE for the Modulation estimation

KDE is a non-parametric approach used heavily in statistics, and it has recently been employed to estimate the PDF, $f(z)$, of an arbitrary random variable $\mathcal{Z}$, based on a finite data sample. KDE has been employed in various applications, including image segmentation, depth map segmentation, tracking in image sequences, blind-source separation, edge enhancement in images, and filtering [24].

In KDE, a pre-defined kernel function is centered at each data sample location. An influence region is defined with the maximum at the data sample location while decreasing in intensity with the distance from that location. A scale parameter, which is also called bandwidth or window width, controls the kernel function that performs smoothing over the surrounding space. Most studies choose the Gaussian function as the kernel function due to its properties of approximation and for having the derivatives of all orders defined over the entire space [24]. In the current study, we also set the kernel function to be Gaussian.

Here, we want to find the PDF of a random variable $\mathcal{Z}$, with PDF $f(z)$, to represent the PDF of either the real or imaginary parts of the received signal, $y(n)$. Since we will be employing Gaussian function as the kernel function, the estimated noise variances will correspond to the bandwidth of the kernel function.

For the received signal with N number received symbols, the PDF of the KDE is given as

$$f(z) = \frac{1}{N} \cdot \sum \mathcal{N}_{pdf}(y(n), \hat{\sigma_w^2}) \tag{3.9}$$

where $\mathcal{N}_{pdf}(y(n), \hat{\sigma_w^2})$ is a normal distribution with mean equal to $y(n)$ and variance equal to the estimated noise variance of the data received, $\hat{\sigma_w^2}$. Note that due to the equiprobable assumption of the constellation points, each individual normal distribution

is taken with equal weight, or $(1/N)$. Also note that $f(z)$ extends from min(x(n)) to max(x(n)).

Fig.3.2 shows the graph of the KDE function, $f(z)$, for a sample signal with modulations 4-QAM , 16-QAM or 64-QAM when SNR is 30 dB.

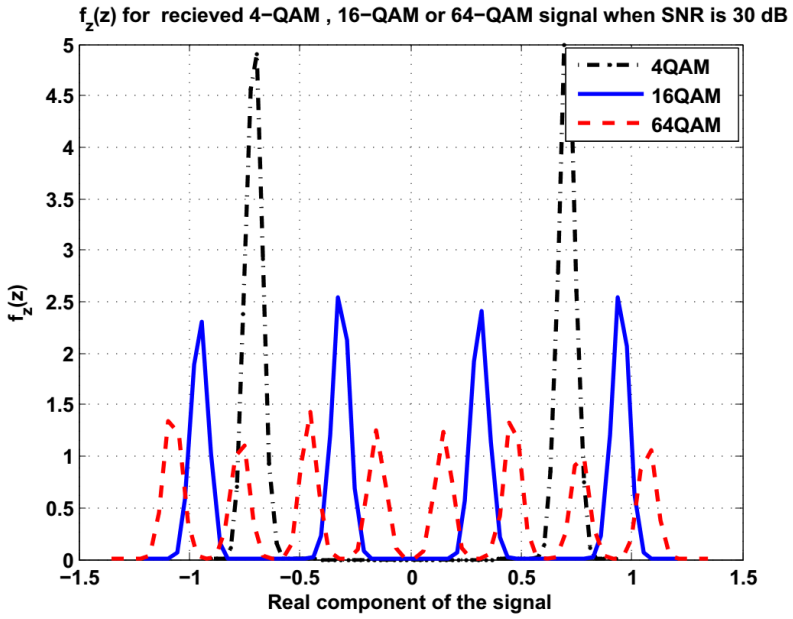

FIGURE 3.2: KDE results of the received signal when the modulation is 4-QAM, 16-QAM, or 64-QAM and when SNR is 30 dB.

3.2.4 Filtering to improve modulation estimation

As we are interested in the peaks of the overall PDF of the KDE function, we are basically interested in the high frequency or sharp changes in the function. Hence, we can perform filtering to eliminate the low frequency parts of the KDE output and will therefore make the estimation process more accurate. This process is performed by a high pass filter (HPF) and its cutoff frequency is chosen according to Figure 3.3. The effect of using the HPFs is shown in Figure 3.4.

Based on the observation and the analytical approaches, a filter with cutoff frequency at 0.2 π is chosen. As shown in Figure 3.3, the estimator performance is the best when a HPF with cutoff frequency at 0.2 π is chosen.

Alternatively, if we take the x-axis of the PDF as the time domain and then observe Discrete Fourier Transform (DFT) of the PDF from the frequency domain point of view,

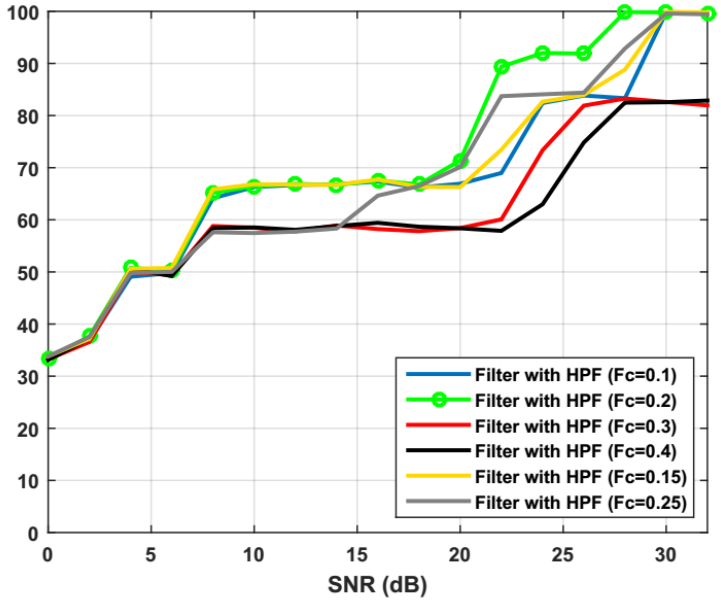

FIGURE 3.3: M-ary classification when changing the HPF parameters prior to estimating the number of peaks (Using 10000 sample test points for different cutoff frequency range from 0.1 to 0.4 (Normalized)).

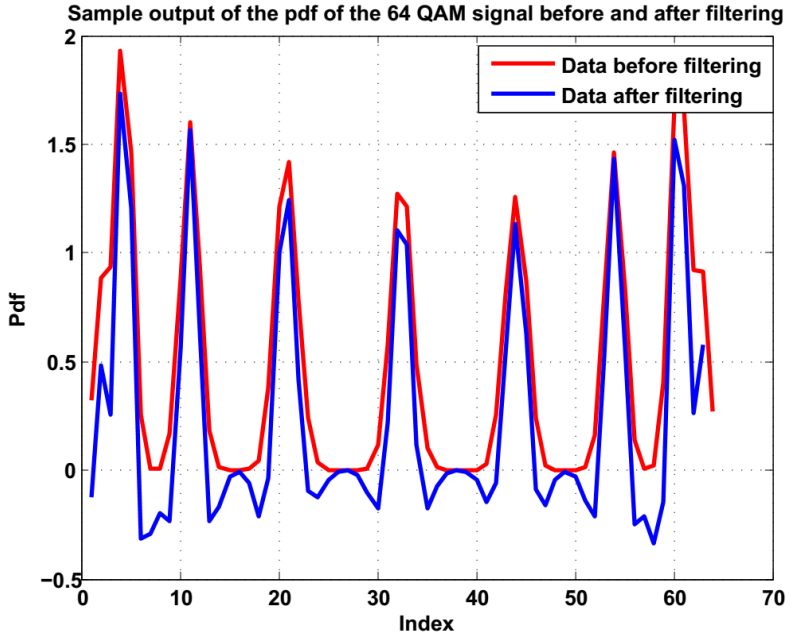

FIGURE 3.4: Filtering effect is shown here by removing the DC and low frequency part of the signal. The peaks are easily identified.

we can see from Fig. 3.5 that we need to remove the low frequency components of the signal and the cutoff frequency agrees with the chosen value.

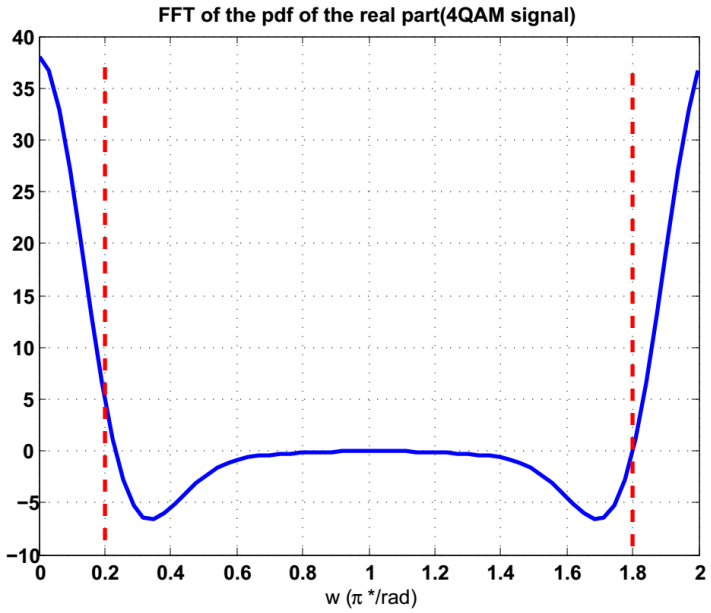

FIGURE 3.5: Frequency domain of a 4-QAM signal(real part)

3.2.5 AMC proposed flow diagram

By combining the approaches presented above, we can define a multi-step process. Below are the steps applied to classify an unknown modulation type:

Modulation estimation process

- **Stage 1**

  1. Start receiving data (Wait until we collect N samples).
  2. Calculate the variance of the absolute of the data received.
  3. Compare the results to a threshold.
  4. If larger: It is QAM modulation , else: It is PSK modulation or 4-QAM.
  5. If PSK:

     – Perform initial classification of 4-QAM and 4-PSK.

     – Prepare the data for PSK M-ary classification (rotation and phase amplification).

6. Else If QAM:

   – Prepare the data for M-ary QAM classification (absolute and shifting).

- **Stage 2**

1. Calculate the estimate of noise variance and then prepare KDE for the data.
2. Filter the KDE output and use the peak detection algorithm to determine the order of the modulation.
3. Determine the modulation type and repeat the process if needed.

Figure 3.6 presents the steps in a flow diagram to make it more clear for the reader.

3.3 Simulation results

3.3.1 Choosing parameters

• Threshold (reference)

We use the variance of the absolute value of the modulated signal since this will reveal the changes in the constellation points when all samples are reflected in one quadrature. We then check the variance to see how different the symbols are from each other. Hence we check $\text{var}(|y(n)|) = \text{var}(|(x(n) + w(n)|)$. Although we can get a mathematical expression for different modulations under a given SNR value as done in [31], and [52], due to the simplicity we prefer to use a graphical approach and get the threshold from the graphic. From the graphs, we can easily find a threshold that will differentiate between QAM and PSK modulations at the beginning of the classification. The approach can also identify higher order QAM modulations from PSK and 4-QAM, since we expect the variance to be larger for the higher order modulations. Hence, by analyzing Figure 3.7, we choose a value of 0.09 for the threshold. For the SNR values smaller than 8 dB, the relation between the SNR and the variance of the absolute of the signal is changing exponentially. However, we can establish a linear relationship for the threshold and the estimated noise

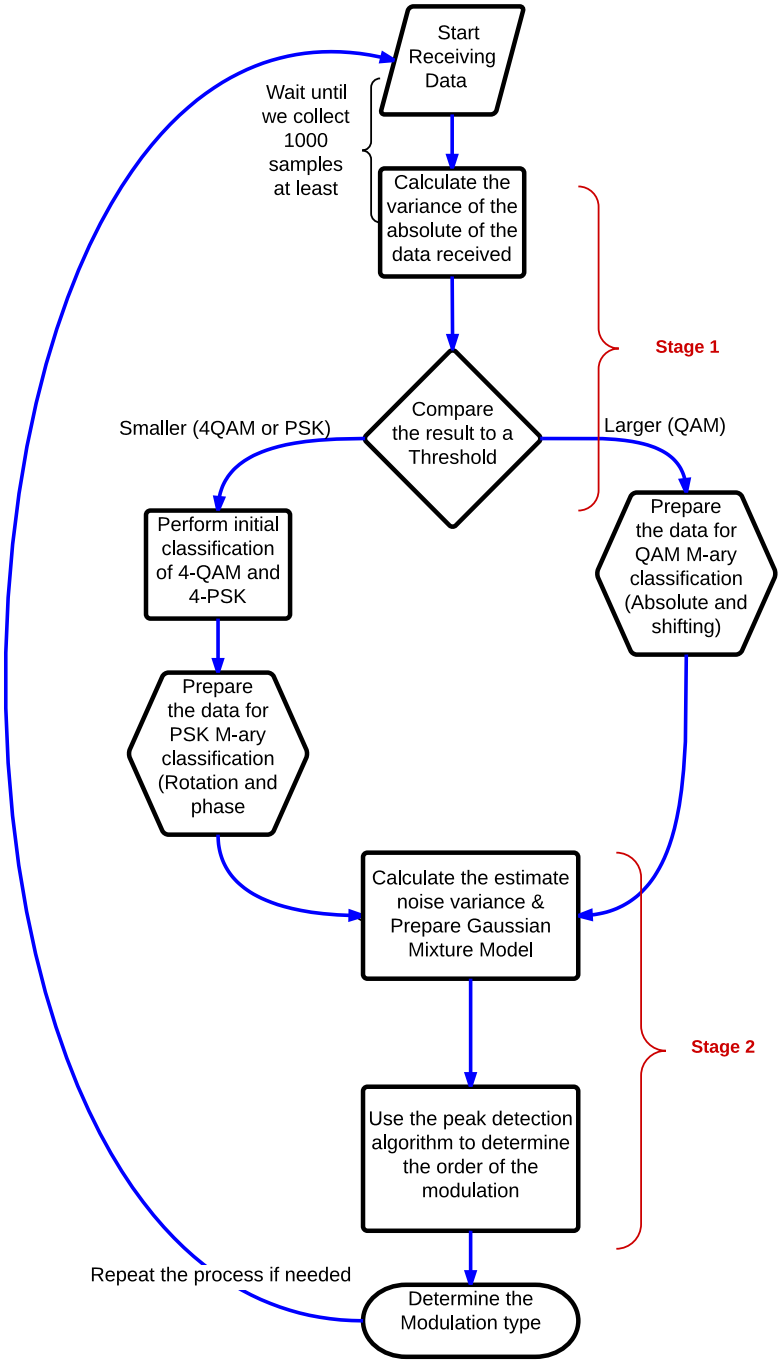

FIGURE 3.6: The flow diagram to illustrates the steps taken to classify the unknown modulation type.

variance. To capture this variation, we used the empirical relation below (Eq. 3.10) for finding the new value of the reference or threshold when SNR is less than 8 dB, or

$$reference = 0.09 + \hat{\sigma_w^2}/4. \tag{3.10}$$

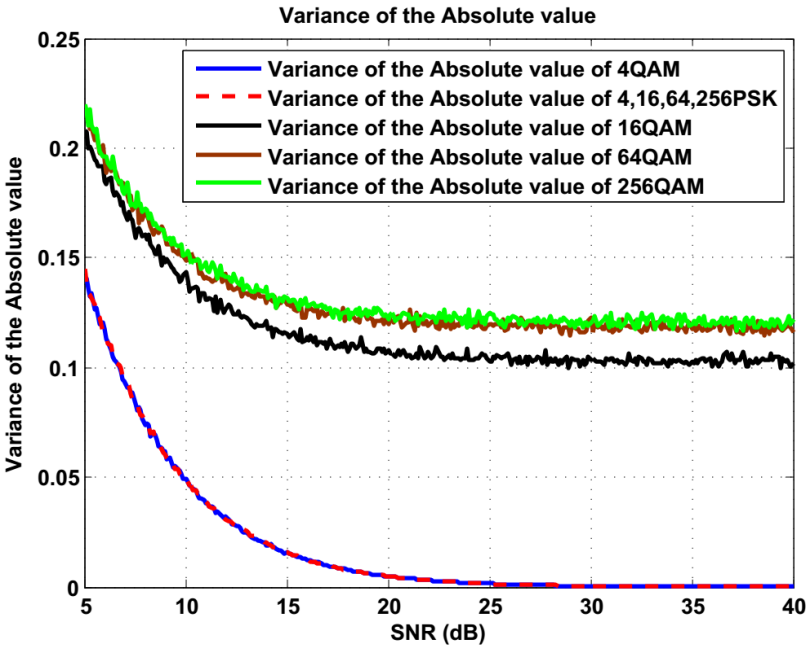

FIGURE 3.7: Variance of absolute QAM and PSK signals with 10000 test cases.

- **Limit 1** (Limit for peak identification)

Since our goal from the beginning of this study is to design a simple classifier, we opted to use a simple window search for finding the peaks. We have also deployed computationally heavy peak detection algorithms but observed that the performance increase was minimal. Hence, we omitted the complicated peak detection algorithms from this study.

Limit 1 is used to choose all the candidate points that might be considered as a peak. Again by observing the curve in Figure 3.8 we choose the value of 0.02 for Limit 1, since with this value the performance of the estimator is found to be the best.

3.3.2 Simulations

Our simulation environment is set up based on the parameters and assumptions below:

1. For AWGN channels, 5,000 symbols are generated for each test case and 100,000 test cases are executed. On the other hand, for fading channels, each test case contains 12,000 symbols and 10,000 test cases are executed.

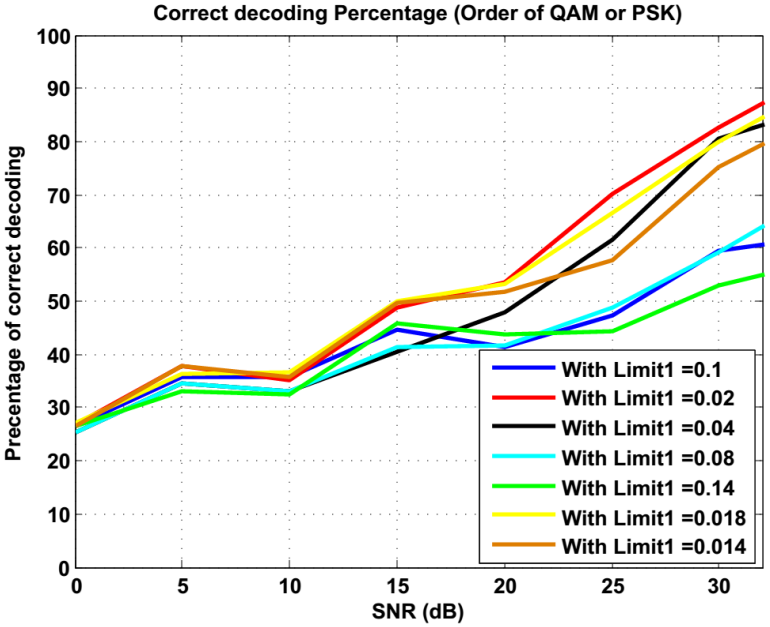

FIGURE 3.8: The selection of Limit 1 based on the best performance.

2. SNRs from 0 to 32 dB in 2 dB step size (typically 32 dB is required for 64 - QAM modulation),

3. 4, 16, and 64 PSK and QAM modulations,

4. HPF cutoff frequency of 0.02 π.

By running the simulations, for the above parameters, we have obtained different figures. For the simulation of each test case, we first generate random binary data, and then modulate it either m-QAM or m-PSK. We then add the random AWGN with a certain power according to the SNR test value. We then apply our algorithm for the estimation of the modulation type used. At the end of the process, for each SNR test value, we assess the performance of the approach of this study by observing two parameters: First we check the percentage of the correct differentiation between PSK and QAM modulations. Secondly, we check the percentage of the correct estimation of the modulation order used.

The results for these two parameters for different SNR values are shown in Figs. 3.9 and 3.10.

Figure 3.9 shows that the differentiation between PSK and QAM modulations was almost perfect when SNR is higher than 10 dB. So the proposed estimator performs very well for practical SNR values. Also as shown in Figure 3.9, in the case of fading channel even with perfect channel compensation the performance degrades.

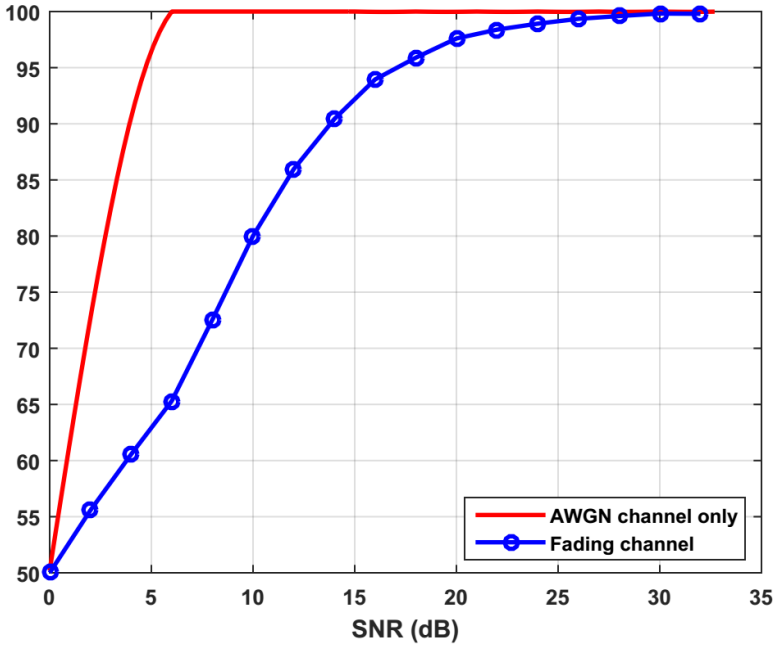

FIGURE 3.9: QAM and PSK differentiation.

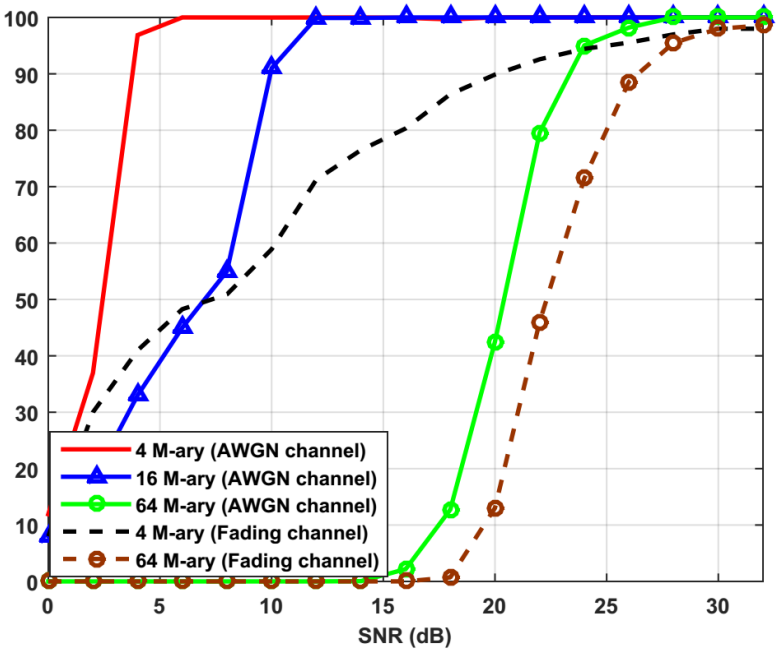

FIGURE 3.10: Determination of the modulation order.

Figure 3.10 shows the detection of the order of the QAM or PSK modulation. It is seen that the proposed solution can differentiate both between QAM and PSK, as well as their orders. As in Figure 3.9 performance of the detection of the order of the QAM or PSK modulation also degrades in the case of fading channel not only AWGN.

From the Figs. 3.9 and 3.10 we can see that as the SNR increases, the detection of the

right peaks in the right places in the PDF becomes more accurate. In Figure 3.10, we further observe that as the modulation order increases, the Euclidean distance between transmitted symbols decreases due to the power normalization. Hence, for the same level of noise signals it is harder to differentiate between different symbols (peaks at real and imaginary parts).

3.3.3 Complexity Analysis

As the prior art does not reveal the number of computations performed for their AMC approach except for some work as in [26] and the fact that the simulation frameworks are different due to different assumptions and modulation techniques, it is hard to have a one-to-one comparison between different studies. Therefore, in this part, we will simply state the complexity of the algorithm proposed by providing general complexity overviews.

With the algorithm presented in this study, we first estimate the noise level and then calculate the variance of the absolute of the signal to decide whether QAM or PSK is used. Then, we use the normal distribution function to implement our estimated KDE output, which is just the addition of the PDFs with a certain weight. After estimating the density function, we need to calculate the number of peaks found in the real and imaginary parts of the signal. This part is accomplished by using a HPF and a comparator to select the peaks. With an additional step, we further remove the near peaks. Finally, we select the best M-ary corresponding to the number of peaks found in density distribution in both the real and imaginary part of the signal received.

We could have developed a more sophisticated algorithm to differentiate QAM from the PSK modulation techniques, but we choose a simple approach as we were targeting a less complex algorithm. Similarly, for peak search algorithm we came up with a basic procedure that gives a good performance. Hence, in general we ended up with a simpler classifier that identifies different QAM and PSK modulation techniques.

Proposed algorithm's complexity analysis:
Assuming that M is the number of the symbols used:

1. PSK or QAM classification step:
   - Calculation of variance of the absolute of the signal needs $M-1$ additions, M abs(complex) and Msquare operations.

• Noise variance estimation needs $2M + 1$ additions and $2M$ square operations.

Total: $3M$ additions, M abs(complex) and $3M$ square operations.

2. M-ary estimation step: Assuming K (64 is used) is the samples needed to represent the PDF (KDE output):

   • In KDE step we need to store values of $\mathcal{N}(0, \hat{\sigma_w^2})$ (Gaussian distribution with mean zero and variance $\hat{\sigma_w^2}$) around 20-30 kernels with K samples each, and calculating the output PDF will cost $K * M$ additions.

   • Filtering:

   Assuming that we use c taps filter (10 taps FIR filter is used), the filtering of the data will cost $c * K$ multiplication and K additions.

   • Peak detection:

   Compare the K values with a limit and removing near peaks will cost around $2K$ comparison and K additions. All this is done for real part of the signal and then repeated for the imaginary part. Hence, this part does not increase the complexity order.

   • Estimating the M-ary from the number of peaks:

   6 additions and 6 comparisons if we have 3 options to choose from (4, 16 and 64 M-ary). Again, this part does not increase the complexity order.

Thus, for the whole classification phase, we have total of :
$3M + 2 * (M + 2) * K$ additions, M abs(complex), $3M$ square, $c * K$ multiplication, and $30 * K$ samples that need to be stored.

3.4 Conclusion

With the integration of the approaches developed in this study, we are able to get promising results with relatively less computation. For example we can differentiate between QPSK, 16-PSK, 64-PSK, 4-QAM, 16-QAM, and 64-QAM modulations with only 1 % of misidentification when the SNR is around the level of minimum requirement of a given modulation. It is observed that this simple efficient technique can find applications in

blind automatic modulation classification as the performance comparison with the state of the art is promising.

Chapter 4

Conclusion and Future Work

Software Defined Radios help to make much or most of the complicated algorithms and techniques that needs to be handled by telecommunications engineers easy and simple. The simplest case for a SDR receiver is to contain simple analog-to-digital converter and RF receiver (antenna). All the filtering, baseband processing, and downconversion can be done digitally, either by using a FPGA or even via a computer connected to a SDR. Nowadays, many researchers are moving from developing and using analog components for high-performance applications towards the idea of using SDR and converting all the processing to the digital domain. Due to the fact that SDR is more flexible for the configuration of a given system, many researchers, who need to build their radio algorithms and test their ideas in realistic environments, are heading towards the use of SDRs and/or similar platforms. That's the reason that in this study we have introduced a channel emulator.

4.1 Channel emulator

For the part of the channel emulator, we proposed an implementation of a fading channel emulator using Clarke/Gans model for the generation of fading channels. We verified the results of the emulator in two stages. First, we checked the frequency spectrum specifications of the channel generated by the channel emulator. Then, we connected an OFDM system running on USRP device to our channel emulator and calculated the BER of the system for different Doppler frequency fading channels. Finally, we compared

the resulting BER curves with theoretical BER floor curves reported in the literature. We have found that our emulator's BER performance was matching with the MATLAB simulation's BER floor, but for the case of theoretical BER floor we needed to add some corrections factors for the f_D and add some ICI error floor.

The BER analysis were done for flat channels for comparison purposes. However, the emulator is capable of emulating multipath channels. To test this, we have emulated a two-path multipath channel. For the simulations, we observed that as the second path power increases the BER increases and the multipath channel act as a flat fading channel when the second path power was very low (-30 dB).

We found that even though our software channel emulator approaches to the performance indicated by the theory, it comes with the price of the latency and low data rates that is compatible with the emulator. As it was hard to use a higher data rate than 200KHz used in step two of the verification. The only way to use high data rates was to use a buffer (memory) to save the channel in.

In addition to the above case, there were some source of impairments due to USRP. Some of the error sources of the USRP platform were fixed directly, while for the others we have used the correction factors. We believe that these errors are the source of the correction factors.

In the end, we have implemented a software channel emulator. This channel emulator can be a very useful and a low-cost tool for other researchers to test their real time systems by using our verified emulator with Doppler effect. Due to the flexibility that LABVIEW m-script offers, the channel emulator can find a range of applications from education to the wireless development activities. The flexibility comes from the point that changing any part of the channel emulator design will only need minor modifications in the LABVIEW m-script.

4.2 Automatic Modulation Classification

An automatic modulation classification scheme for a group of digitally modulated signals, such as QPSK, 16-PSK, 64-PSK, 4-QAM, 16-QAM, and 64-QAM modulations by employing the Kernel Density Estimation function for the probability distribution of real

and imaginary parts of a modulated signal is proposed. To simplify the complexity of the detection, the classification is done in two stages: First, classification between QAM and PSK signals is performed, and then the M-ary order is determined by developing the KDE for the data and using a simple peak detection algorithm. The simulation results showed that the classification can identify the modulation types when the SNR of the signal is in the typical levels of a given modulation. Hence, an alternative modulation detection approach is offered with a low-complexity. The proposed method here is further improved when adaptive change in the classification parameters with respect to the SNR levels is introduced. With little modifications on the decision criteria, the proposed method can be used for digitally modulated amplitude shift keying (ASK) signals. As for the frequency shift keying (FSK) and minimum shift keying (MSK) modulation techniques, alternative approaches will need to be developed. For systems that operate in multipath channels, the current work can be exploited when the multipath components are identified.

As can be seen from the approaches given, building algorithms on the platforms that enable software based approaches makes the life of wireless designer much easier. The easy to change configurations and experiments that can be performed in the lab instead of the outdoor field experiments are the invaluable gadgets that a wireless designer engineer can seek. With the algorithms provided in this thesis, a small step is provided towards these dreams. More will be realized with the development of new algorithms.

4.3 Publications

Our study on the AMC was accepted by the Canadian Journal of Electrical and Computer Engineering on summer 2016 and is published by IEEE. Our efforts on the channel emulator are also put into a conference paper for potential publication. Below are the details of these two papers:

- H. Abuella and M. K. Ozdemir, "Automatic Modulation Classification Based on Kernel Density Estimation," in Canadian Journal of Electrical and Computer Engineering, vol. 39, no. 3, pp. 203-209, Summer 2016 (oi: 10.1109/CJECE.2016.2570250).
- H. Abuella and M. K. Ozdemir, "Real-time fading channel emulator using SDR with theoretical verification", to be submitted for conference publication.

Appendix A

Proof for equation 2.4 used to calculate the BER for a given fading channel with certain f_D

Assuming that channel gain g is constant over OFDM symbol T. This assumption is invalid for invalid for fixed R_s and increasing of Doppler frequency. In this proof we will show that variations in g_k over the OFDM N sub-carriers will cause ICI. This ICI will behave like additional AWGN and will cause an error floor at high SNRs.

After receiving the OFDM symbol with N symbols at the receiver and after the FFT block the received sub-carriers and after removal of the G guard band symbols are as follow:

$$Z_{n,i} = \sqrt{\frac{2 * E_h}{T}} H(0) X_{n,i} + C_{n,i} \tag{A.1}$$

where $X_{n,i}$ is the sent symbols, $H(0)$ is the effective complex channel gain, E_h is the avg. energy of the channel and $C_{n,i} = \sum_{m=0, m\neq i}^{N-1} X_{n,m} H(m-i)$. Where $H(m-i)$ is function of g_k:

$$H(m-i) = \sum_{k=0}^{N-1} g_{G+(k-G)_N} \mathbf{e}^{\frac{j2\pi(m-i)k}{N}} \tag{A.2}$$

Note that in case of time invariant channel g is constant and $Z_{n,i} = g\sqrt{\frac{2*E_h}{T}} X_{n,i}$.

So we want to find the ICI part ($C_{n,i}$) and calculate its energy. For high N we can assume that $C_{n,i}$ is a complex Gaussian random variable. Since $X_{n,m}$ and $H(m-i)$ are independent RVs, and $E[X_{n,m}] = 0$, So $E[C_l] = 0$.

Since,

$$2E_h = E_{av}\delta_{km}$$

So we get the auto-correlation of the ICI part as:

$$\phi_{cc}(r) = \frac{1}{2}E[C_{n,i}C^*_{n,i+r}]$$
$$= \frac{E_{av}}{T}\sum_{m\neq i,i+r} E[H(m-i)H^*(m-i-r)]$$

To proceed further we need to get the time correlation of the channel. First, we need to make some assumptions:

1. $E[|g_k|^2] = 1$ (normalization of the channel).
2. Clarke's 2D isotropic scattering model with isotropic scattering model with isotropic receiver antenna.

Finally we get the auto-correlation of the ICI term :

$$\phi_{cc}(r) = \frac{E_{av}}{T}\delta_r - \frac{E_{av}}{TN^2}\sum_{k=0}^{N-1}\sum_{k^l=0}^{N-1} J_o(2\pi f_m T(k-k^l))(\mathbf{e}^{\frac{j2\pi k^l r}{N}} + (1-\delta_r)\mathbf{e}^{\frac{j2\pi kr}{N}})$$

To find the variance of the ICI (σ^2_{ICI}) let r=0, So we get :

$$\phi_{cc}(0) = \frac{E_{av}}{T} - \frac{E_{av}}{TN^2}(N + 2\sum_{i=0}^{N-1}(N-i)J_o(2\pi f_D T i))$$

Finally we find the SIR with a simple equation :

$$SIR = \frac{E_{av}/T}{\phi_{cc}(0)}$$

we can find the BER floor for any modulation scheme using the SIR.

Appendix B

LABVIEW diagram used to generate the curves in Figure 2.14

In Figure B.1 we present the user interface of the LABVIEW VI. Then, in Figure B.2 we present the block diagram of the LABVEIW VI.

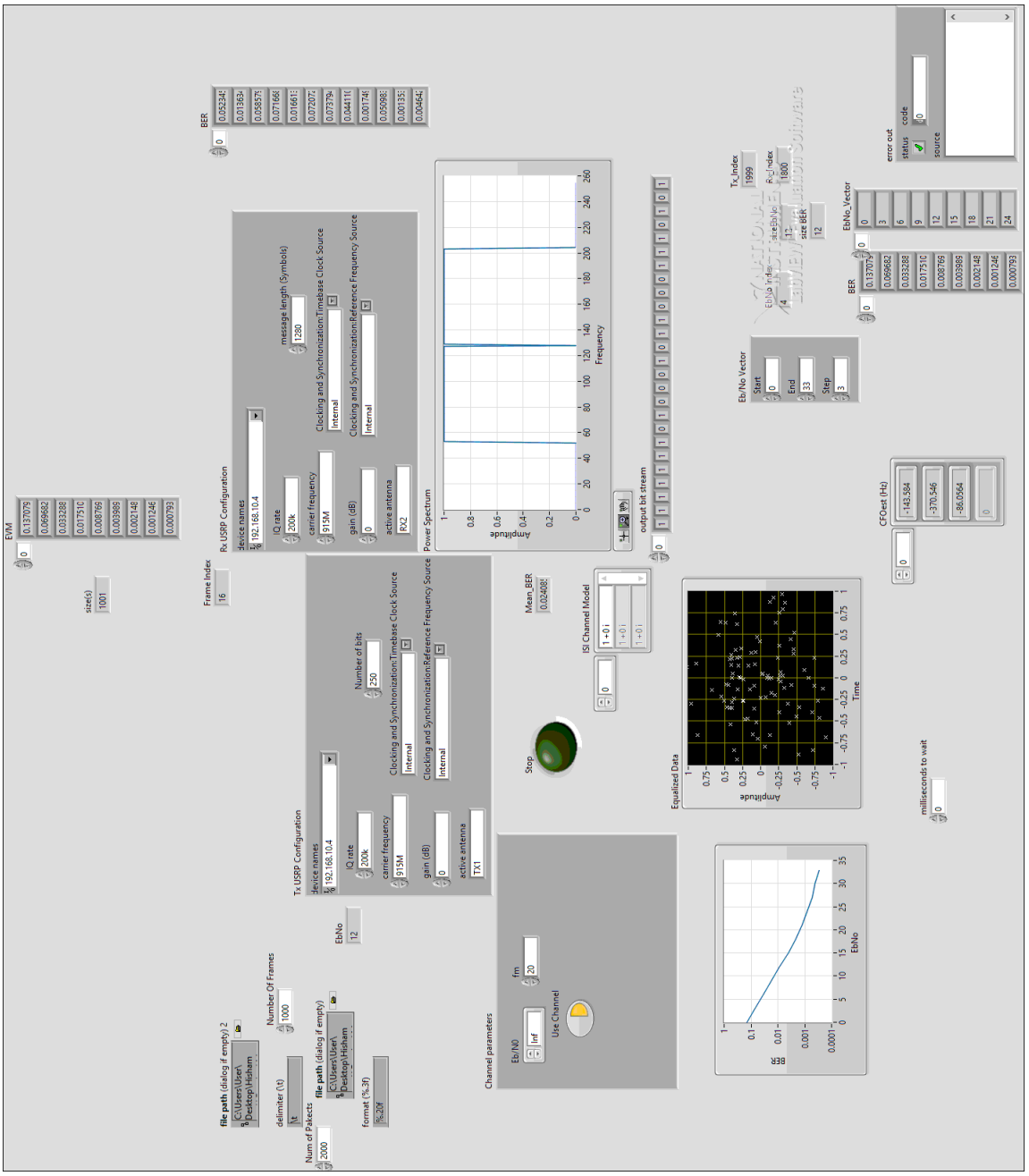

FIGURE B.1: The user interface of the VI used to generate the BER curves.

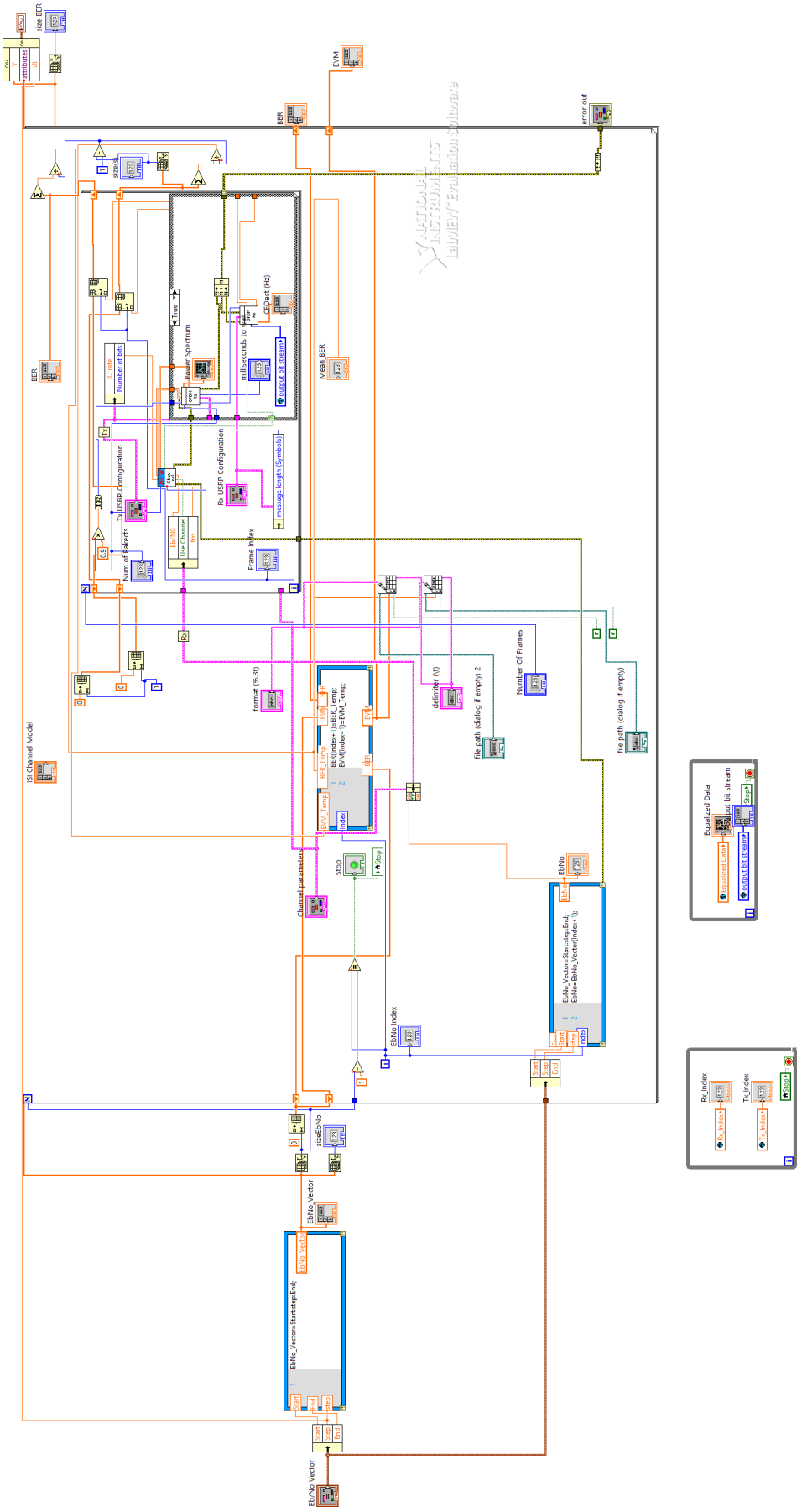

FIGURE B.2: The block diagram to illustrates the VI used to generate the BER curves.

Bibliography

[1] S. Dowling, "An example of a univariate (one dimensional) Gaussian mixture model , [online]," http://dirichletprocess.weebly.com/clustering, Accessed 2016-11-20. [Online]. Available: http://dirichletprocess.weebly.com/clustering

[2] J. Mar, C. C. Kuo, Y. R. Lin, and T. H. Lung, "Design of software-defined radio channel simulator for wireless communications: Case study with DSRC and UWB channels," *IEEE Transactions on Instrumentation and Measurement*, vol. 58, no. 8, pp. 2755–2766, Aug 2009.

[3] D. Vlastaras, S. Malkowsky, and F. Tufvesson, "Stress test of vehicular communication transceivers using software defined radio," in *2015 IEEE 81st Vehicular Technology Conference (VTC Spring)*, May 2015, pp. 1–4.

[4] H. C. Bui and L. Franck, "Cost effective emulation of geostationary satellite channels by means of software-defined radio," in *Metrology for Aerospace (MetroAeroSpace), 2014 IEEE*, May 2014, pp. 538–542.

[5] G. Ghiaasi, M. Ashury, D. Vlastaras, M. Hofer, Z. Xu, and T. Zemen, "Real-time vehicular channel emulator for future conformance tests of wireless its modems," in *2016 10th European Conference on Antennas and Propagation (EuCAP)*, April 2016, pp. 1–5.

[6] J. J. Olmos, A. Gelonch, F. J. Casadevall, and G. Femenias, "Design and implementation of a wide-band real-time mobile channel emulator," *IEEE Transactions on Vehicular Technology*, vol. 48, no. 3, pp. 746–764, May 1999.

[7] K. Prahlad and B. Ramamurthi, "Design and implementation of a multi-terminal channel emulator on LTE testbed," in *Communications (NCC), 2015 Twenty First National Conference on*, Feb 2015, pp. 1–6.

[8] J. Matai, P. Meng, L. Wu, B. Weals, and R. Kastner, "Designing a hardware in the loop wireless digital channel emulator for software defined radio," in *Field-Programmable Technology (FPT), 2012 International Conference on*, Dec 2012, pp. 206–214.

[9] A. D. Fontaine, E. Salt, and D. E. Dodds, "A multipath channel emulator integrated with a QAM modulator," in *Electrical and Computer Engineering (CCECE), 2013 26th Annual IEEE Canadian Conference on*, May 2013, pp. 1–4.

[10] C. C. Fu, T. P. Wang, K. C. Chang, C. H. Liao, and T. D. Chiueh, "A real-time digital baseband channel emulation system for OFDM communications," in *APCCAS 2006 - 2006 IEEE Asia Pacific Conference on Circuits and Systems*, Dec 2006, pp. 984–987.

[11] A. Patnaik, A. Talebzadeh, M. Tsiklauri, D. Pommerenke, C. Ding, D. White, S. Scearce, and Y. Yang, "Implementation of a 18 ghz bandwidth channel emulator using an FIR filter," in *2014 IEEE International Symposium on Electromagnetic Compatibility (EMC)*, Aug 2014, pp. 950–955.

[12] S. Haene, D. Perels, and W. Fichtner, "System-level characterization of a real-time MIMO-OFDM transceiver on FPGA," in *Signal Processing Conference, 2007 15th European*, Sept 2007, pp. 1146–1150.

[13] S. Yang and Z. Can, "Design and implementation of multiple antenna channel emulator for LTE system," in *Communications and Networking in China (CHINACOM), 2014 9th International Conference on*, Aug 2014, pp. 208–213.

[14] T. M. Fernandez-Carames, M. G. Lopez, and L. Castedo, "Fpga-based vehicular channel emulator for evaluation of ieee 802.11p transceivers," in *Intelligent transport systems telecommunications,(ITST),2009 9th International Conference on*, Oct 2009, pp. 592–597.

[15] O. Dobre, A. Abdi, Y. Bar-Ness, and W. Su, "Survey of automatic modulation classification techniques: classical approaches and new trends," *Communications, IET*, vol. 1, no. 2, pp. 137–156, April 2007.

[16] O. A. Dobre, A. Abdi, Y. Bar-Ness, and W. Su, "Blind modulation classification: a concept whose time has come," in *IEEE/Sarnoff Symposium on Advances in Wired and Wireless Communication, 2005.*, April 2005, pp. 223–228.

[17] E. Rebeiz, F.-L. Yuan, P. Urriza, D. Markovic, and D. Cabric, "Energy-efficient processor for blind signal classification in cognitive radio networks," *Circuits and Systems I: Regular Papers, IEEE Transactions on*, vol. 61, no. 2, pp. 587–599, 2014.

[18] J. Xu, W. Su, and M. Zhou, "Likelihood-ratio approaches to automatic modulation classification," *Systems, Man, and Cybernetics, Part C: Applications and Reviews, IEEE Transactions on*, vol. 41, no. 4, pp. 455–469, July 2011.

[19] J. Sills, "Maximum-likelihood modulation classification for PSK/QAM," in *Military Communications Conference Proceedings, 1999. MILCOM 1999. IEEE*, vol. 1, 1999, pp. 217–220 vol.1.

[20] J. Liu, X. Wang, J. Nadeau, and H. Lin, "Modulation classification based on Gaussian mixture models under multipath fading channel," in *Global Communications Conference (GLOBECOM), 2012 IEEE*, Dec 2012, pp. 3970–3974.

[21] M. W. Aslam, Z. Zhu, and A. K. Nandi, "Automatic modulation classification using combination of genetic programming and KNN," *Wireless Communications, IEEE Transactions on*, vol. 11, no. 8, pp. 2742–2750, August 2012.

[22] Z. Yaqin, R. Guanghui, W. Xuexia, W. Zhilu, and G. Xuemai, "Automatic digital modulation recognition using artificial neural networks," in *Neural Networks and Signal Processing, 2003. Proceedings of the 2003 International Conference on*, vol. 1, Dec 2003, pp. 257–260 Vol.1.

[23] W. Juan-ping, H. Ying-zheng, Z. Jin-mei, and W. Hua-kui, "Automatic modulation recognition of digital communication signals," in *Pervasive Computing Signal Processing and Applications (PCSPA), 2010 First International Conference on*, Sept 2010, pp. 590–593.

[24] A. Bors and N. Nasios, "Kernel bandwidth estimation for nonparametric modeling," *Systems, Man, and Cybernetics, Part B: Cybernetics, IEEE Transactions on*, vol. 39, no. 6, pp. 1543–1555, Dec 2009.

[25] A. Zhang and Y. Wei, "Modulation recognition of decision tree svm based on chaotic particle swarm [j]," *Video Engineering*, vol. 23, p. 037, 2012.

[26] P. Urriza, E. Rebeiz, P. Pawelczak, and D. Cabric, "Computationally efficient modulation level classification based on probability distribution distance functions," *IEEE Communications Letters*, vol. 15, no. 5, pp. 476–478, May 2011.

[27] A. Swami and B. Sadler, "Hierarchical digital modulation classification using cumulants," *Communications, IEEE Transactions on*, vol. 48, no. 3, pp. 416–429, Mar 2000.

[28] X. Zhou, Y. Wu, and B. Wang, "The MPSK signals modulation classification based on kernel methods," in *Antennas, Propagation and EM Theory, 2008. ISAPE 2008. 8th International Symposium on.* IEEE, 2008, pp. 1419–1422.

[29] X. Zhou, G. Yang, and Y. Wu, "Digital modulation classification using kernel fisher discriminant analysis for reconfigurable software radio," in *Signal Processing, 2008. ICSP 2008. 9th International Conference on.* IEEE, 2008, pp. 2001–2004.

[30] S. Fki, A. Aissa-El-Bey, and T. Chonavel, "Blind equalization and automatic modulation classification based on PDF fitting," in *Acoustics, Speech and Signal Processing (ICASSP), 2015 IEEE International Conference on.* IEEE, 2015, pp. 2989–2993.

[31] Q. Shi and Y. Karasawa, "Automatic modulation identification based on the probability density function of signal phase," *IEEE Transactions on Communications*, vol. 60, no. 4, pp. 1033–1044, April 2012.

[32] A. I. Fontes, L. A. Pasa, V. A. de Sousa, J. A. Costa, L. F. Silveira, and F. Abinader, "Automatic modulation classification using information theoretic similarity measures," in *Vehicular Technology Conference (VTC Fall), 2012 IEEE.* IEEE, 2012, pp. 1–5.

[33] X. Zhou, Y. Wu, and G. Yang, "Modulation classification of MPSK signals based on relevance vector machines," in *Information Engineering and Computer Science, 2009. ICIECS 2009. International Conference on.* IEEE, 2009, pp. 1–5.

[34] M. H. Valipour, M. M. Homayounpour, and M. A. Mehralian, "Automatic digital modulation recognition in presence of noise using SVM and PSO," in *Telecommunications (IST), 2012 Sixth International Symposium on.* IEEE, 2012, pp. 378–382.

[35] H. Zhang, H. Liao, and L. Gan, "Robust classification of quadrature amplitude modulation constellations based on GMM," in *Communication Problem-Solving (ICCP), 2014 IEEE International Conference on*, Dec 2014, pp. 546–549.

[36] Recom, "Wireless EM propagation software (wireless insite) website, [online]," http://www.remcom.com/wireless-insite, Accessed 2016-10-20. [Online]. Available: http://www.remcom.com/wireless-insite

[37] T. S. Rappaport, *Wireless communications: principles and practice (2nd Edition)*, 2nd ed. Prentice Hall, 2002.

[38] R. H. Clarke, "A statistical theory of mobile-radio reception," *Bell System Technical Journal*, vol. 47, no. 6, pp. 957–1000, 1968. [Online]. Available: http://dx.doi.org/10.1002/j.1538-7305.1968.tb00069.x

[39] J. Mitola, "Software radio architecture: a mathematical perspective," *IEEE Journal on Selected Areas in Communications*, vol. 17, no. 4, pp. 514–538, Apr 1999.

[40] N. Instruments, "NI-USRP details," www.ni.com/sdr/usrp/, 2016. [Online]. Available: www.ni.com/sdr/usrp/

[41] N. I. examples, "Real-time MIMO channel emulation on the ni pxie-5644r, [online]," http://www.ni.com/example/31556/en/, May 2013. [Online]. Available: http://www.ni.com/example/31556/en/

[42] S. Communications, "Sr5500 channel emulator, [online]," https://www.spirent.com/, Accessed 2016-9-20. [Online]. Available: https://www.spirent.com/

[43] K. Technologies, "Propsim channel emulation, [online]," http://www.keysight.com/, Accessed 2016-9-20. [Online]. Available: http://www.keysight.com/

[44] J. I. Smith, "A computer generated multipath fading simulation for mobile radio," *IEEE Transactions on Vehicular Technology*, vol. 24, no. 3, pp. 39–40, Aug 1975.

[45] J. J. van de Beek, M. Sandell, and P. O. Borjesson, "Ml estimation of time and frequency offset in OFDM systems," *IEEE Transactions on Signal Processing*, vol. 45, no. 7, pp. 1800–1805, Jul 1997.

[46] G. L. S. (auth.), *Principles of mobile communication*, 3rd ed. Springer-Verlag New York, 2012.

[47] M. N. S. S. Ke-Lin Du, *Wireless communication systems: From RF subsystems to 4G enabling technologies.* Cambridge University Press, 2010.

[48] *NI USRP-292x/293x Datasheet*, National Instruments , 8 2015. [Online]. Available: http://www.ni.com/datasheet/pdf/en/ds-355

[49] B. Ramkumar, T. Bose, and M. S. Radenkovic, "Combined blind equalization and automatic modulation classification for cognitive radios," in *Digital Signal Processing Workshop and 5th IEEE Signal Processing Education Workshop, 2009. DSP/SPE 2009. IEEE 13th*, Jan 2009, pp. 172–177.

[50] S. Kharbech, I. Dayoub, M. Zwingelstein-Colin, E. P. Simon, and K. Hassan, "Blind digital modulation identification for time-selective MIMO channels," *IEEE Wireless Communications Letters*, vol. 3, no. 4, pp. 373–376, Aug 2014.

[51] T. B. B. Ramkumar and M. Radenkovic, "Robust automatic modulation classification and blind equalization: novel cognitive receivers," *Analog Integrated Circuits and Signal Processing*, vol. 69, no. 2-3, pp. 271–281, 2011.

[52] S. S. Soliman and S. Z. Hsue, "Signal classification using statistical moments," *IEEE Transactions on Communications*, vol. 40, no. 5, pp. 908–916, May 1992.

[53] O. Dobre, M. Oner, S. Rajan, and R. Inkol, "Cyclostationarity-based robust algorithms for QAM signal identification," *Communications Letters, IEEE*, vol. 16, no. 1, pp. 12–15, January 2012.

[54] C. Weber, M. Peter, and T. Felhauer, "Automatic modulation classification technique for radio monitoring," *Electronics Letters*, vol. 51, no. 10, pp. 794–796, 2015.

[55] C. Cardoso, A. R. Castro, and A. Klautau, "An efficient FPGA IP core for automatic modulation classification," *IEEE Embedded Systems Letters*, vol. 5, no. 3, pp. 42–45, Sept 2013.

[56] D. Digdarsini, M. Kumar, G. Khot, T. V. S. Ram, and V. K. Tank, "FPGA implementation of automatic modulation recognition system for advanced SATCOM system," in *Signal Processing and Integrated Networks (SPIN), 2014 International Conference on*, Feb 2014, pp. 464–469.

[57] J. L. Xu, W. Su, and M. Zhou, "Software-defined radio equipped with rapid modulation recognition," *IEEE Transactions on Vehicular Technology*, vol. 59, no. 4, pp. 1659–1667, May 2010.